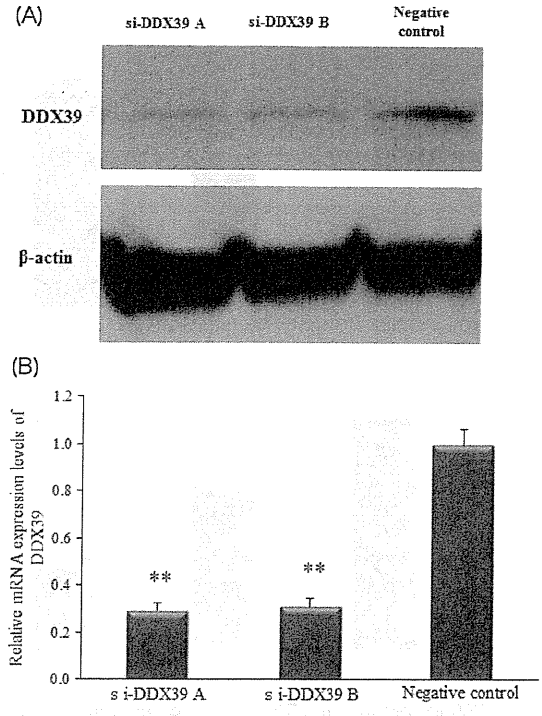

Fig. 4. Two siRNAs for DDX39 (si-DDX39 A and si-DDX39 B) down-regulated the protein (A) and mRNA expression of DDX39 (B). **P < 0.01.

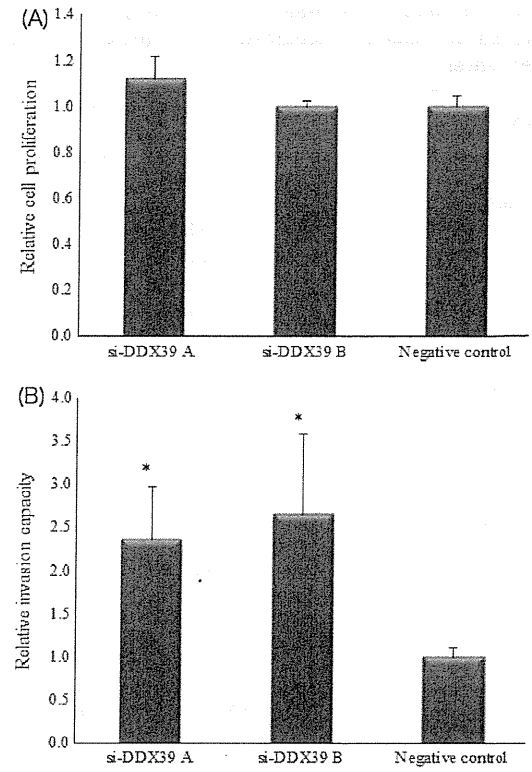

Fig. 5. siRNA knockdown effects on cell proliferation and invasion ability using T24 bladder cancer cells. (A) No significant difference in cell proliferation was found between si-DDX39 transfected cells and control cells. (B) Cells transfected with si-DDX39 A and si-DDX39 B gained significantly higher invasion ability compared to control cells. *P < 0.05.

DDX39 had prognostic value for predicting progression of NMIBCs.

In conclusion, our results suggest that DDX39 is a suppressor of invasion and could be a useful molecular marker for predicting progression of urothelial carcinoma and a novel target for clinical therapy.

Acknowledgments

We are grateful to Rie Onodera, Kaori Nakakubo, Azusa Inagaki, Keiko Sakata, and Yuko Hisabayashi (Osaka City University, Osaka, Japan) for their technical assistance, to Yukiko Iura (Osaka City University) for her assistance in the preparation of this manuscript, and to Dr. Samuel M. Cohen (University of Nebraska Medical Center, Omaha, NE, USA) for reviewing this manuscript. This work was supported in part by a grant from the Ministry of Health, Labor and Welfare of Japan.

Disclosure Statement

The authors have no conflict of interest.

References

1 Jemal A, Siegel R, Xu J, Ward E. Cancer statistics, 2010. *CA Cancer J Clin* 2010; 60: 277–300.
2 Epstein JI, Amin MB, Reuter VR, Mostofi FK. The World Health Organization/International Society of Urological Pathology consensus classification of urothelial (transitional cell) neoplasms of the urinary bladder. Bladder Consensus Conference Committee. *Am J Surg Pathol* 1998; 22: 1435–48.
3 Rubben H, Lutzeyer W, Fischer N, Deutz F, Lagrange W, Giani G. Natural history and treatment of low and high risk superficial bladder tumors. *J Urol* 1988; 139: 283–5.
4 Thurman SA, DeWeese TL. Multimodality therapy for the treatment of muscle-invasive bladder cancer. *Semin Urol Oncol* 2000; 18: 313–22.
5 Althausen AF, Prout GR Jr, Daly JJ. Non-invasive papillary carcinoma of the bladder associated with carcinoma in situ. *J Urol* 1976; 116: 575–80.
6 Herr HW. Tumor progression and survival of patients with high grade, non-invasive papillary (TaG3) bladder tumors: 15-year outcome. *J Urol* 2000; 163: 60–1; discussion 1–2.
7 Habuchi T, Marberger M, Droller MJ *et al.* Prognostic markers for bladder cancer: International Consensus Panel on bladder tumor markers. *Urology* 2005; 66: 64–74.
8 Esrig D, Spruck CH III, Nichols PW *et al.* p53 nuclear protein accumulation correlates with mutations in the p53 gene, tumor grade, and stage in bladder cancer. *Am J Pathol* 1993; 143: 1389–97.
9 Goebell PJ, Groshen SG, Schmitz-Drager BJ. p53 immunohistochemistry in bladder cancer–a new approach to an old question. *Urol Oncol* 2010; 28: 377–88.
10 Kamai T, Takagi K, Asami H, Ito Y, Oshima H, Yoshida KI. Decreasing of p27(Kip1) and cyclin E protein levels is associated with progression from superficial into invasive bladder cancer. *Br J Cancer* 2001; 84: 1242–51.
11 Korkolopoulou P, Christodoulou P, Konstantinidou AE, Thomas-Tsagli E, Kapralos P, Davaris P. Cell cycle regulators in bladder cancer: a multivariate survival study with emphasis on p27Kip1. *Hum Pathol* 2000; 31: 751–60.
12 Letarte S, Brusniak MY, Campbell D *et al.* Differential plasma glycoproteome of p19 skin cancer mouse model using the corra label-free LC-MS proteomics platform. *Clin Proteomics* 2008; 4: 105.
13 Tsui KH, Tang P, Lin CY, Chang PL, Chang CH, Yung BY. Bikunin loss in urine as useful marker for bladder carcinoma. *J Urol* 2010; 183: 339–44.
14 Kirkali Z, Chan T, Manoharan M *et al.* Bladder cancer: epidemiology, staging and grading, and diagnosis. *Urology* 2005; 66: 4–34.
15 Sui J, Zhang J, Tan TL, Ching CB, Chen WN. Comparative proteomics analysis of vascular smooth muscle cells incubated with S- and R-enantiomers of

doi: 10.1111/j.1349-7006.2012.02298.x

atenolol using iTRAQ-coupled two-dimensional LC-MS/MS. *Mol Cell Proteomics* 2008; 7: 1007–18.
16 Palou J, Algaba F, Vera I, Rodriguez O, Villavicencio H, Sanchez-Carbayo M. Protein expression patterns of ezrin are predictors of progression in T1G3 bladder tumours treated with nonmaintenance bacillus Calmette–Guerin. *Eur Urol* 2009; 56: 829–36.
17 Tsui KH, Juang HH, Lee TH, Chang PL, Chen CL, Yung BY. Association of nucleophosmin/B23 with bladder cancer recurrence based on immunohistochemical assessment in clinical samples. *Acta Pharmacol Sin* 2008; 29: 364–70.
18 Tzai TS, Tsai YS, Shiau AL, Wu CL, Shieh GS, Tsai HT. Urine prothymosin-alpha as novel tumor marker for detection and follow-up of bladder cancer. *Urology* 2006; 67: 294–9.
19 Higgins JP, Kaygusuz G, Wang L *et al.* Placental S100 (S100P) and GATA3: markers for transitional epithelium and urothelial carcinoma discovered by complementary DNA microarray. *Am J Surg Pathol* 2007; 31: 673–80.
20 Pryor A, Tung L, Yang Z, Kapadia F, Chang TH, Johnson LF. Growth-regulated expression and G0-specific turnover of the mRNA that encodes URH49, a mammalian DExH/D box protein that is highly related to the mRNA export protein UAP56. *Nucleic Acids Res* 2004; 32: 1857–65.
21 Sugiura T, Sakurai K, Nagano Y. Intracellular characterization of DDX39, a novel growth-associated RNA helicase. *Exp Cell Res* 2007; 313: 782–90.
22 Abdelhaleem M. Over-expression of RNA helicases in cancer. *Anticancer Res* 2004; 24: 3951–3.
23 Sugiura T, Nagano Y, Noguchi Y. DDX39, upregulated in lung squamous cell cancer, displays RNA helicase activities and promotes cancer cell growth. *Cancer Biol Ther* 2007; 6: 957–64.
24 Lipponen PK, Eskelinen MJ. Reduced expression of E-cadherin is related to invasive disease and frequent recurrence in bladder cancer. *J Cancer Res Clin Oncol* 1995; 121: 303–8.
25 Kumar B, Koul S, Petersen J *et al.* p38 mitogen-activated protein kinase-driven MAPKAPK2 regulates invasion of bladder cancer by modulation of MMP-2 and MMP-9 activity. *Cancer Res* 2010; 70: 832–41.
26 Babjuk M, Oosterlinck W, Sylvester R, Kaasinen E, Bohle A, Palou-Redorta J. EAU guidelines on non-muscle-invasive urothelial carcinoma of the bladder. *Eur Urol* 2008; 54: 303–14.
27 Sakano S, Matsuyama H, Takai K *et al.* Risk group stratification to predict recurrence after transurethral resection in Japanese patients with stage Ta and T1 bladder tumours: validation study on the European Association of Urology guidelines. *BJU Int* 2011; 107: 1598–604.

J Toxicol Pathol 2012; 25: 209–214

Original Article

Lack of Hepatocarcinogenicity of Combinations of Low Doses of 2-amino-3, 8-dimethylimidazo[4,5-*f*]quinoxaline and Diethylnitrosamine in Rats: Indication for the Existence of a Threshold for Genotoxic Carcinogens

Min Wei[1], Anna Kakehashi[1], Shotaro Yamano[1], Seiko Tamano[2], Tomoyuki Shirai[3], Hideki Wanibuchi[1*] and Shoji Fukushima[1,4*]

[1] Department of Pathology, Osaka City University Graduate School of Medicine, 1-4-3 Asahi-machi, Abeno-ku, Osaka 545-8585, Japan
[2] DIMS Institute of Medical Science, Inc., 64 Goura, Nishiazai, Azai-cho, Ichinomiya 491-0113, Japan
[3] Department of Experimental Pathology and Tumor Biology, Nagoya City, University Graduate School of Medical Sciences, 1 Kawasumi, Mizuho-cho, Mizuho-ku, Nagoya 467-8601, Japan
[4] Japan Bioassay Research Center, 2445 Hirosawa, Hadano, Kanagawa 257-0015, Japan

Abstract: The purposes of the present study were to evaluate the hepatocarcinogenicity of concurrent treatment of 2-amino-3,8-dimethylimidazo[4,5-*f*]quinoxaline (MeIQx) and diethylnitrosamine (DEN) in rats and to determine whether no effect levels of combinations of these two different structural categories of genotoxic hepatocarcinogens exist. Two 16-week rat hepatocarcinogenesis assays were performed using a total of 790 male F344 rats. In experiment 1, we evaluated the effects of concurrent treatment of a subcarcinogenic dose of DEN on rat hepatocarcinogenesis induced by various doses of MeIQx. In experiment 2, we determined hepatocarcinogenicities of combinations of MeIQx and DEN at subcarcinogenic doses, low carcinogenic doses and high carcinogenic doses. Quantitative analyses of glutathione *S*-transferase placental form (GST-P)-positive foci, a preneoplastic lesion of the liver in rats, revealed that concurrent treatment with subcarcinogenic doses of DEN did not enhance MeIQx-induced rat hepatocarcinogenicity. We also found that concurrent treatment with combinations of subcarcinogenic doses of DEN and MeIQx was not hepatocarcinogenic, indicating that the combined effects of subcarcinogenic doses of DEN and MeIQx were neither additive nor synergistic. Moreover, concurrent treatment with low carcinogenic doses of these 2 carcinogens did not show additive or synergistic effects. Synergetic effects were observed only in rats coadministered high carcinogenic doses of the 2 carcinogens. These results demonstrate the existence of no effect levels of combinations of these 2 genotoxic hepatocarcinogens, and provide new evidence supporting our idea that there is a threshold, at least a practical threshold, that should be considered when evaluating the risk of genotoxic carcinogens. (DOI: 10.1293/tox.25.209; J Toxicol Pathol 2012; 25: 209–214)

Key words: MeIQx, DEN, concurrent treatment, carcinogenic threshold, low dose carcinogenicity

Introduction

Exposure to environmental carcinogens is one of the most significant causes of human cancers. Determination of the dose-response relationship between carcinogen exposure and induction of cancer is one of the most important areas of chemical risk assessment. It is generally assumed that genotoxic carcinogens exert a non-threshold carcinogenic effect. This concept, however, is being challenged, as advancements in the understanding of the molecular mechanisms of carcinogenesis are being made and experimental evidence continues to accumulate showing that individual genotoxic carcinogens do not exert mutagenic or carcinogenic effects at low doses[1–6]. Given the probability that humans are exposed concurrently or sequentially to trace concentrations of multiple environmental carcinogens, examination of the effects of combinations of low doses of genotoxic carcinogens is an indispensable part of cancer risk assessment.

Previous studies of carcinogenic responses in rats exposed simultaneously to multiple carcinogens indicated that additive or synergistic effects were usually evident at high exposure levels of carcinogens, but this was not always the case at low carcinogen levels (reviewed by Shirai T[7]). For example, concurrent treatment with low doses of 3 *N*-nitro-

Received: 23 April 2012, Accepted: 14 June 2012
*Corresponding authors: S Fukushima (e-mail: s-fukushima@jisha.or.jp), H Wanibuchi (e-mail: wani@med.osaka-cu.ac.jp)

so compounds (genotoxic carcinogens) did not show additive effects on liver tumor development; only treatment with high doses exerted an additive effect[8]. Furthermore, concurrent treatment with low doses of 5 or 10 heterocyclic amines did not enhance development of preneoplastic lesions of the liver either additively or synergistically when given at the post-initiation stage in medium-term live bioassays (Ito test)[9–11]. These findings suggested that concurrent treatment with genotoxic carcinogens at low doses did not necessarily entail additive risk for carcinogenicity[7].

The effects of combinations of different structural categories of genotoxic carcinogens, e.g., combinations of heterocyclic amines and *N*-nitroso compounds, have not been evaluated. It also should be noted that the studies mentioned above focused mainly on the enhanced carcinogenic effects of combinations of multiple carcinogens and did not address the issue of threshold. Using various carcinogenesis models in different rat strains, we have demonstrated the existence of no effect levels for the hepatocarcinogenicity of 2-amino-3,8-dimethylimidazo[4,5-*f*]quinoxaline (MeIQx), a genotoxic heterocyclic amine contained in seared fish and meat, and also for diethylnitrosamine (DEN), a genotoxic *N*-nitroso compound synthesized in the stomach through the reaction of secondary amines and nitrites in the diet[1]. The purposes of the present study were to evaluate the hepatocarcinogenicity of the concurrent treatment of MeIQx and DEN in rats and to determine whether no effect levels of combinations of these two genotoxic hepatocarcinogens exist.

Materials and Methods

Chemicals and diets

MeIQx (purity, 99.9%) was purchased from the Nard Institute (Nishinomiya, Japan), and DEN (purity>99.5%) was purchased from Sakai Research Laboratory (Fukui, Japan). Basal diet (powdered MF, Oriental Yeast Co., Ltd., Tokyo, Japan) and diets containing MeIQx were prepared once a month by Oriental Yeast Co., Ltd., Japan.

Animals

A total of 790 male F344 rats were supplied from Charles River Laboratories Japan, Inc. (Shiga, Japan) and were used at 21 days of age. Animals were housed in polycarbonate cages (5 rats/cage) in experimental animal rooms with a targeted temperature of 22 ± 3 °C, relative humidity of 55 ± 5% and a 12-h light/dark cycle. Diet and tap water were available *ad libitum* throughout the study. Fresh diet and drinking water were supplied to the animals twice weekly. Body weights, food consumption and water intake were measured weekly.

Experimental protocols

Animal experiment protocols were approved by the Institutional Animal Care and Use Committee of Osaka City University Medical School.

Experiment 1 was designed to evaluate the effects of subcarcinogenic doses of DEN on MeIQx-induced rat hepatocarcinogenesis. A total of 400 rats were randomized into 12 groups and treated with test chemicals for 16 weeks as shown in the Table 1. Group 1 was the control group without administration of any of test compounds. Groups 2–6 were MeIQx-alone treatment groups that were fed diets containing MeIQx at doses of 0.01, 0.1, 1, 10, and 100 ppm, respectively. Group 7 was the DEN-alone treatment group that was administered 0.01 ppm DEN in the drinking water. Groups 8–12 were the concurrent treatment groups coadministered the above doses of MeIQx and 0.01 ppm DEN. MeIQx dose selection was based on the results of a previous low-dose MeIQx hepatocarcinogenicity study; in that study, hepatocarcinogenic effects were not observed at doses of 1 ppm MeIQx and below[12]. The dose of 0.01 ppm for DEN was the maximum noncarcinogenic dose observed in a previous low-dose DEN hepatocarcinogenicity study[12]. The treatment period of 16 weeks was the same as in our previous low-dose carcinogenicity studies[1]. All rats were killed at the end of week 16 under deep anesthesia. At necropsy, livers were excised and weighed, and then 3 slices each from the left lateral, medial, and right lateral lobes were cut and placed in 10% phosphate buffered formalin. Following fixa-

Table 1. Final Body and Liver Weights, and Intakes of Test Chemicals (Experiment 1)

Group	MeIQx (ppm)	DEN (ppm)	No. of rats	Total intake of MeIQx (mg/kg bw)	Total intake of DEN (mg/kg bw)	Body weight (g)	Liver weights	
							Absolute (g)	Relative (%)
1	—	—	40	0	0	321 ± 13	9.54 ± 0.54	2.97 ± 0.11
2	0.01	—	40	0.07	0	332 ± 15 [a]	9.79 ± 0.59	2.95 ± 0.11
3	0.1	—	40	0.71	0	338 ± 16 [a]	9.83 ± 0.63	2.91 ± 0.09
4	1	—	40	7.11	0	332 ± 14 [a]	9.76 ± 0.66	2.94 ± 0.13
5	10	—	30	71.82	0	332 ± 17 [a]	9.94 ± 0.64 [a]	2.99 ± 0.10
6	100	—	10	720.79	0	325 ± 21	11.17 ± 0.88 [a]	3.44 ± 0.08 [a]
7	—	0.01	40	0	0.095	327 ± 15	9.67 ± 0.58	2.95 ± 0.09
8	0.01	0.01	40	0.07	0.093	344 ± 18 [a,b]	9.80 ± 0.59 [a]	2.85 ± 0.08 [a,b]
9	0.1	0.01	40	0.69	0.093	340 ± 16 [a,b]	9.79 ± 0.61	2.88 ± 0.10 [a,b]
10	1	0.01	40	6.86	0.095	341 ± 21 [a,b]	9.84 ± 0.74 [a]	2.89 ± 0.12 [a,b]
11	10	0.01	30	70.42	0.095	326 ± 14	9.78 ± 0.70	2.99 ± 0.13
12	100	0.01	10	704.20	0.093	323 ± 14	11.01 ± 0.48 [a,b]	3.41 ± 0.05 [a,b]

—, 0 ppm in the diet or drinking water. [a] Significantly different from group 1. [b] Significantly different from the respective MeIQx-alone group.

tion, liver tissues were embedded in paraffin and processed for histopathological examination and immunohistochemical analysis of glutathione *S*-transferase placental form (GST-P)-positive foci, a well-established preneoplastic liver lesion in rats that can extend the range of the observable effect levels of a carcinogen and has been accepted as a reliable and sensitive end-point marker in assessment of the carcinogenic effects of environmentally relevant concentrations of carcinogens[1,7,13].

Experiment 2 was designed to evaluate the hepatocarcinogenicities of combinations of MeIQx and DEN at subcarcinogenic doses, low carcinogenic doses and high carcinogenic doses. A total of 390 male F344 rats were randomized into 16 groups and treated with test chemicals for 16 weeks as shown in Table 3. Group 1 was the control group without administration of any test compounds. Groups 2–6 were MeIQx-alone treatment groups that were administered increasing doses of MeIQx as in Experiment 1. Groups 7–11 were DEN-alone treatment groups that were administered DEN in the drinking water at doses of 0.0001, 0.001, 0.01, 0.1 and 1 ppm. The DEN dosages in this study were the same as used in previous low-dose DEN hepatocarcinogenicity studies[12]. Groups 12–16 were coadministered MeIQx and DEN as follows: subcarcinogenic dose combination groups were administered 0.01 ppm MeIQx + 0.0001 ppm DEN (group 12), 0.1 ppm MeIQx + 0.001 ppm DEN (group 13) or 1 ppm MeIQx + 0.01 ppm DEN (group 14); the low carcinogenic dose combination group was administered 10 ppm MeIQx + 1 ppm DEN (group 15); and the high carcinogenic dose combination group was administered 100 ppm MeIQx + 10 ppm DEN (group 16). At the end of week 16, all rats were necropsied, and livers were processed and analyzed as in Experiment 1.

Examination of GST-P-positive foci in the liver

Anti-rat GST-P polyclonal antibody (Medical and Biological Laboratories Co., Ltd., Nagoya, Japan) at a dilution of 1:1000 was used for immunohistochemical staining of GST-P. GST-P-positive hepatocellular foci composed of 2 or more cells were counted under a light microscope[2,12,14,15]. Total areas of livers were measured using an IPAP color image processor (Sumica Technos, Osaka, Japan), and the number of GST-P-positive foci per square centimeter of liver tissue was calculated.

Statistical analysis

All mean values are reported as means ± SD. Statistical analyses were performed using the StatLight program (Yukms Co., Ltd., Tokyo, Japan) as described previously[2,14,16]. Briefly, homogeneity of variance was tested by the F test or Bartlett's test. Differences in mean values between the control and MeIQx- or DEN-alone treatment groups were evaluated by the 2-tailed Dunnett test when the variance was homogeneous and the 2-tailed Steel test when the variance was heterogeneous. Differences in mean values between the MeIQx- or DEN-alone groups and their respective concurrent treatment groups, and between concurrent treatment groups and the control group were evaluated by the 2-tailed Student's test when the variance was homogeneous and the 2-tailed Welch's *t* test when the variance was heterogeneous. P values less than 0.05 were considered significant.

Results

Experiment 1

The final average body and liver weights and test chemical intakes are summarized in Table 1. In the MeIQx-alone treatment groups, the final body weights of the 0.01, 0.1, 1 and 10 ppm MeIQx groups were slightly but statistically significantly higher than that of the control group (non-treatment group). Consequently, a significant increase in absolute liver weights but not the relative liver weights was observed in the 10 ppm MeIQx group compared with the control group. There was an apparent treatment-related increase in liver weight in the 100 ppm MeIQx group, as evidenced by the findings that the final body weights of this group did not significantly differ from that of the control group but both the absolute and relative liver weights were significantly increased. There were no significant differences in body weight or absolute or relative liver weight between the MeIQx-alone groups and their respective MeIQx + 0.01 ppm DEN groups. Since 0.01 ppm DEN (group 7) had no effect on body or liver weight compared with the control group, the changes in body and liver weights observed in the MeIQx + 0.01 ppm DEN groups compared with the control groups were attributed to MeIQx treatment. The intake of DEN was similar among DEN treatment groups, and the intake of MeIQx was proportional to the administered doses (Table 1). No histopathological changes were observed in the livers of any of the groups.

Total numbers of GST-P-positive foci, composed of 2 or more cells (Fig. 1), per unit area of the rat liver are shown in Table 2. In the MeIQx-alone treatment groups, the numbers of GST-P-positive foci in the livers of groups administered 0.01 ppm to 10 ppm of MeIQx did not differ from the non-treatment control value. In contrast, a significant increase was observed in the group administered 100 ppm MeIQx. As expected, 0.01 ppm DEN did not increase the number of GST-P-positive foci; in fact, the number of GST-P-positive foci in this group showed a slight but significant decrease compared with the control group. There were no significant differences in the numbers of GST-P-positive foci between the groups receiving combinations of MeIQx and 0.01 ppm DEN and their respective MeIQx-alone groups. Importantly, the numbers of GST-P-positive foci in the livers of the groups receiving combinations of 0.01 ppm to 10 ppm of MeIQx and 0.01 ppm DEN did not differ from the control value. These results indicate that the subcarcinogenic dose of 0.01 ppm DEN did not exert either additive or synergistic effects on MeIQx-induced hepatocarcinogenesis in rats.

Experiment 2

The final average body and liver weights and test chemical intakes are summarized in Table 3. MeIQx-alone

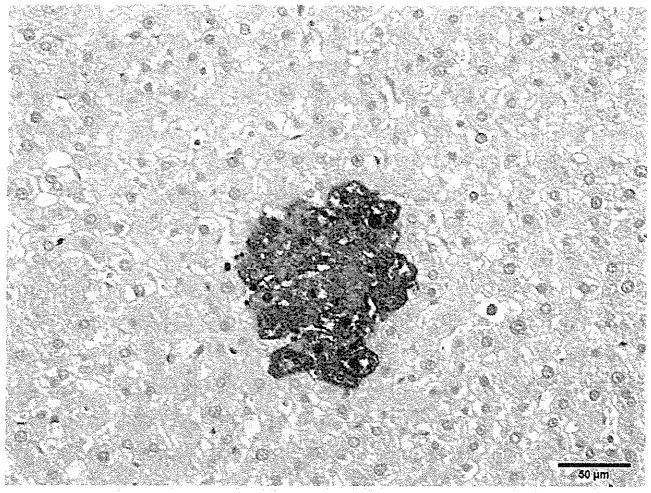

Fig. 1. GST-P-positive focus in the liver of a rat administered 100 ppm MeIQx + 1 ppm DEN (Experiment 2).

Table 2. GST-P-positive Foci in the Rat Liver (Experiment 1)

Group	MeIQx (ppm)	DEN (ppm)	No. of rats	GST-P-positive foci (no./cm^2)
1	—	—	40	0.11 ± 0.23
2	0.01	—	40	0.08 ± 0.18
3	0.1	—	40	0.10 ± 0.20
4	1	—	40	0.15 ± 0.24
5	10	—	30	0.17 ± 0.23
6	100	—	10	10.7 ± 3.97 [a]
7	—	0.01	40	0.03 ± 0.12 [a]
8	0.01	0.01	40	0.05 ± 0.14
9	0.1	0.01	40	0.10 ± 0.20
10	1	0.01	40	0.14 ± 0.26
11	10	0.01	30	0.16 ± 0.27
12	100	0.01	10	12.21 ± 7.07 [a, b]

—, 0 ppm in the diet or drinking water. [a] Significantly different from group 1. [b] Significantly different from the 100 ppm MeIQx-alone group.

Table 3. Final Body and Liver Weights, and Intakes of Test Chemicals (Experiment 2)

Group	MeIQx (ppm)	DEN (ppm)	No. of rats	Total intake of MeIQx (mg/kg bw)	Total intake of DEN (mg/kg bw)	Body weight (g)	Liver weights	
							Absolute (g)	Relative (%)
1	—	—	30	0	0	326 ± 13	8.99 ± 0.43	2.76 ± 0.10
2	0.01	—	30	0.06	0	327 ± 33	8.90 ± 0.99	2.72 ± 0.11
3	0.1	—	30	0.58	0	335 ± 15	9.30 ± 0.46 [a]	2.77 ± 0.09
4	1	—	30	5.65	0	330 ± 19	9.08 ± 0.62	2.75 ± 0.12
5	10	—	20	61.58	0	332 ± 12	9.47 ± 0.43 [a]	2.85 ± 0.11 [a]
6	100	—	10	623.29	0	326 ± 9	10.40 ± 0.48 [a]	3.19 ± 0.09 [a]
7	—	0.0001	30	0	0.001	319 ± 14	8.87 ± 0.49	2.78 ± 0.16
8	—	0.001	30	0	0.010	324 ± 15	9.20 ± 0.55	2.84 ± 0.09 [a]
9	—	0.01	30	0	0.096	315 ± 27	8.90 ± 0.74	2.83 ± 0.14
10	—	0.1	20	0	0.937	322 ± 15	9.17 ± 0.63	2.85 ± 0.15
11	—	1	10	0	10.220	317 ± 12	9.16 ± 0.55	2.89 ± 0.09 [a]
12	0.01	0.0001	30	0.06	0.001	340 ± 13 [a, b]	9.13 ± 0.46 [b]	2.69 ± 0.09 [a, b]
13	0.1	0.001	30	0.58	0.010	336 ± 13 [a, b]	9.40 ± 0.58 [a]	2.80 ± 0.12
14	1	0.01	30	5.60	0.097	334 ± 14 [a, b]	9.18 ± 0.51	2.75 ± 0.08 [b]
15	10	0.1	20	59.61	0.999	333 ± 27	9.55 ± 0.86 [a]	2.87 ± 0.09 [a]
16	100	1	10	625.68	9.655	331 ± 12 [b]	10.55 ± 0.72 [a, b]	3.19 ± 0.12 [a, b]

—, 0 ppm in the diet or drinking water. [a] Significantly different from group 1. [b] Significantly different from the respective DEN-alone group.

and DEN-alone treatments had no effect on body weights compared with the control group. No body weight suppression was observed in any combination treatment group. The final body weights of the 0.01 ppm MeIQx + 0.0001 ppm DEN, 0.1 ppm MeIQx + 0.001 ppm DEN, 1 ppm MeIQx + 0.01 ppm DEN and 100 ppm MeIQx + 1 ppm DEN treatment groups were significantly higher than their respective DEN-alone groups. Apparent treatment-related increases in both absolute and relative liver weights were observed in the groups administered 10 and 100 ppm MeIQx-alone and the groups administered 10 ppm MeIQx + 0.1 ppm DEN and 100 ppm MeIQx + 1 ppm DEN. The intake of DEN and MeIQx was proportional to the administered doses (Table 3). No histopathological changes were observed in the livers of any of the groups.

The numbers of GST-P-positive foci in rat livers are shown in Table 4. The numbers of GST-P-positive foci in the groups administered 0.01 ppm to 1 ppm MeIQx and in the groups administered 0.0001 to 0.01 ppm DEN did not differ from the non-treatment control group. Furthermore, the numbers of GST-P-positive foci in the groups administered combinations of subcarcinogenic doses of MeIQx and DEN (0.01 ppm MeIQx + 0.0001 ppm DEN, 0.1 ppm MeIQx + 0.001 ppm DEN and 1 ppm MeIQx + 0.01 ppm DEN groups) did not differ from either their respective single treatment groups or the non-treatment control group.

In the MeIQx- and DEN-alone treatment groups, significant increases in the numbers of GST-P-positive foci were observed in the groups administered 10 ppm and 100 ppm MeIQx and in the groups administered 0.1 ppm and 1 ppm DEN. However, there was no significant difference in the number of GST-P-positive foci between the 10 ppm MeIQx + 0.1 ppm DEN group and the 10 ppm MeIQx-alone or 0.1 ppm DEN-alone groups, indicating that the hepatocar-

Table 4. GST-P-positive Foci in the Rat Liver (Experiment 2)

Group	MeIQx (ppm)	DEN (ppm)	No. of rats	GST-P-positive foci (no./cm2)
1	-	—	30	0.20 ± 0.32
2	0.01	—	30	0.17 ± 0.27
3	0.1	—	30	0.24 ± 0.30
4	1	—	30	0.21 ± 0.28
5	10	—	20	0.57 ± 0.51 [a]
6	100	—	10	13.76 ± 8.78 [a]
7	—	0.0001	30	0.30 ± 0.40
8	—	0.001	30	0.29 ± 0.39
9	—	0.01	30	0.35 ± 0.48
10	—	0.1	20	0.82 ± 0.77 [a]
11	—	1	10	8.28 ± 4.27 [a]
12	0.01	0.0001	30	0.36 ± 0.48
13	0.1	0.001	30	0.17 ± 0.24
14	1	0.01	30	0.34 ± 0.51
15	10	0.1	20	0.78 ± 0.70 [a]
16	100	1	10	33.81 ± 17.46 [a,b,c]

—, 0 ppm in the diet or drinking water. [a] Significantly different from group 1. [b] Significantly different from the 100 ppm MeIQx-alone group. [c] Significantly different from the 1 ppm DEN-alone group.

cinogenicity of a combination of low carcinogenic doses of these two carcinogens was not enhanced additively or synergistically. In contrast, the number of GST-P-positive foci in the high carcinogenic dose combination group, the 100 ppm MeIQx + 1 ppm DEN group, was synergistically increased compared with the single treatment groups.

Discussion

The present study demonstrates that concurrent treatment with subcarcinogenic doses of DEN did not enhance MeIQx-induced rat hepatocarcinogenesis. We also found that concurrent treatment with combinations of subcarcinogenic doses of DEN and MeIQx were not hepatocarcinogenic, indicating that the combined effects of subcarcinogenic doses of DEN and MeIQx were neither additive nor synergistic. Moreover, concurrent treatment with low carcinogenic doses of DEN and MeIQx did not show either additive or synergistic effects. Only in rats coadministered higher carcinogenic doses of DEN and MeIQx were synergistic effects seen. The present study provides the first experimental data on the carcinogenic effects of concurrent exposure to subcarcinogenic doses of genotoxic carcinogens belonging to different structural categories. The findings of this study are in line with previous studies on the carcinogenic effects of mixtures of chemicals[7], and provide new evidence supporting our idea that no effect levels for genotoxic carcinogens exist[1,2]. Taking into account the accumulating evidence suggesting the existence of no effect levels for genotoxic carcinogens, it is reasonable to assume that the dose-response curves of genotoxic carcinogens do not reach zero in a physiologically meaningful manner, and that threshold, at least practical threshold, doses exist for the carcinogenicity of genotoxic carcinogens.

Although several threshold mechanisms for genotoxic carcinogens have been suggested, including induction of detoxification processes, cell cycle delay, DNA repair, and apoptosis and the suppression of neoplastically transformed cells by the immune system[3,17–19], the exact mechanisms are anticipated to be complicated and remain to be elucidated. This is especially true for combinations of multiple genotoxic carcinogens. We recently found that induction of $p21^{Cip/WAF1}$ and DNA repair enzymes such as AP endonuclease-1 (APE1) and GADD45 are at least partially responsible for the observed noncarcinogenic effect of low doses of 2-amino-3-methylimidazo[4,5-*f*]quinolone, a genotoxic heterocyclic amine, in rat livers[2]. Further studies are needed to clarify whether similar mechanisms contribute to the noncarcinogenic effect of low doses of MeIQx and/or DEN by evaluating the expression of genes involved in cell proliferation, DNA repair, metabolic activation and apoptosis.

Although combinations of carcinogens are generally considered to act in an additive or synergistic way with respect to cancer risk, recently it has been shown that carcinogens may interact in a non-syncarcinogenic way and, indeed, sometimes interact in an anticarcinogenic way, especially if they do not have a similar mode of carcinogenic action[7,20,21]. As reviewed by Ruediger H[21], interactive mechanisms by which one carcinogen may antagonize or attenuate the carcinogenic action of another carcinogen include inhibition of metabolic activation of procarcinogens, induction of metabolic inactivation, slowing down of the cell cycle via the p53 pathway, interference with the generation of DNA-adducts, and induction of apoptosis. The fact that concurrent treatment with low carcinogenic doses of MeIQx and DEN did not show additive or synergistic effects while combinations of the 2 carcinogens showed synergistic effects at higher carcinogenic doses suggests that combinations of MeIQx and DEN do not exert carcinogenicity in a simple dose-dependent manner and also indicates the possibility of antagonistic interaction between these 2 carcinogens when administered at low doses. Further research to clarify the interactive mechanisms mentioned above will not only facilitate the understanding of the carcinogenicity of combinations of MeIQx and DEN, but will also expand the understanding of threshold mechanisms.

In conclusion, the present study demonstrated that concurrent treatment with noncarcinogenic doses of DEN and MeIQx did not exert hepatocarcinogenicity in rats and that their combined effects were neither additive nor synergistic. These findings further support our idea that there is a threshold, at least a practical threshold, that should be considered when evaluating the risk of genotoxic carcinogens. Dose-response relationships for low dose genotoxic carcinogens, especially for mixtures of carcinogens, are still controversial in the field of carcinogen risk assessment. Further accumulation of data, especially mechanistic data, should be promoted to facilitate not only our understanding of the carcinogenic effects of low doses of genotoxic carcinogens, but also to establish accurate means of risk assessment.

Acknowledgments: The authors would like to acknowledge the encouragement of Dr. N. Ito (the late Prof. Emeritus, Nagoya City University Medical School, Nagoya, Japan) and Dr. T. Kitagawa (Director Emeritus, the Cancer Institute of Japanese Foundation for Cancer Research, Tokyo). This research was supported by a grant from the Project of Core Research for Evolutional Science and Technology (CREST), Japan.

References

1. Fukushima S, Wei M, Kakehashi A, and Wanibuchi H. Cancer Risk Assessment, Thresholds for Genotoxic Carcinogens: Evidence from Mechanism –Based Carcinogenicity Studies. John Wiley and Sons, Inc., 2010.
2. Wei M, Wanibuchi H, Nakae D, Tsuda H, Takahashi S, Hirose M, Totsuka Y, Tatematsu M, and Fukushima S. Low-dose carcinogenicity of 2-amino-3-methylimidazo[4,5-f] quinoline in rats: Evidence for the existence of no-effect levels and a mechanism involving p21(Cip/WAF1). Cancer Sci. **102**: 88–94. 2011. [Medline] [CrossRef]
3. Sofuni T, Hayashi M, Nohmi T, Matsuoka A, Yamada M, and Kamata E. Semi-quantitative evaluation of genotoxic activity of chemical substances and evidence for a biological threshold of genotoxic activity. Mutat Res. **464**: 97–104. 2000. [Medline]
4. Williams GM, Iatropoulos MJ, and Jeffrey AM. Mechanistic basis for nonlinearities and thresholds in rat liver carcinogenesis by the DNA-reactive carcinogens 2-acetylaminofluorene and diethylnitrosamine. Toxicologic pathology. **28**: 388–395. 2000. [Medline] [CrossRef]
5. Waddell WJ, Fukushima S, and Williams GM. Concordance of thresholds for carcinogenicity of N-nitrosodiethylamine. Archives of toxicology. **80**: 305–309. 2006. [Medline] [CrossRef]
6. Waddell WJ. Thresholds of carcinogenicity in the ED01 study. Toxicological Sciences. **72**: 158–163. 2003. [Medline] [CrossRef]
7. Shirai T, Ogawa K, and Takahashi S. Carcinogenic Effects of mixtures of chemicals. J Toxicol Pathol. **19**: 1–13. 2006. [CrossRef]
8. Berger MR, Schmahl D, and Zerban H. Combination experiments with very low doses of three genotoxic N-nitrosamines with similar organotropic carcinogenicity in rats. Carcinogenesis. **8**: 1635–1643. 1987. [Medline] [CrossRef]
9. Hasegawa R, Shirai T, Hakoi K, Takaba K, Iwasaki S, Hoshiya T, Ito N, Nagao M, and Sugimura T. Synergistic enhancement of glutathione S-transferase placental form-positive hepatic foci development in diethylnitrosamine-treated rats by combined administration of five heterocyclic amines at low doses. Jpn J Cancer Res. **82**: 1378–1384. 1991. [Medline] [CrossRef]
10. Ito N, Hasegawa R, Shirai T, Fukushima S, Hakoi K, Takaba K, Iwasaki S, Wakabayashi K, Nagao M, and Sugimura T. Enhancement of GST-P positive liver cell foci development by combined treatment of rats with five heterocyclic amines at low doses. Carcinogenesis. **12**: 767–772. 1991. [Medline] [CrossRef]
11. Hasegawa R, Kato T, Hirose M, Takahashi S, Shirai T, and Ito N. Enhancement of hepatocarcinogenesis by combined administration of food-derived heterocyclic amines at low doses in the rat. Food Chem Toxicol. **34**: 1097–1101. 1996. [Medline] [CrossRef]
12. Fukushima S, Wanibuchi H, Morimura K, Wei M, Nakae D, Konishi Y, Tsuda H, Uehara N, Imaida K, Shirai T, Tatematsu M, Tsukamoto T, Hirose M, Furukawa F, Wakabayashi K, and Totsuka Y. Lack of a dose-response relationship for carcinogenicity in the rat liver with low doses of 2-amino-3,8-dimethylimidazo[4,5-f]quinoxaline or N-nitrosodiethylamine. Jpn J Cancer Res. **93**: 1076–1082. 2002. [Medline] [CrossRef]
13. Tsuda H, Fukushima S, Wanibuchi H, Morimura K, Nakae D, Imaida K, Tatematsu M, Hirose M, Wakabayashi K, and Moore MA. Value of GST-P positive preneoplastic hepatic foci in dose-response studies of hepatocarcinogenesis: evidence for practical thresholds with both genotoxic and non-genotoxic carcinogens. A review of recent work. Toxicol Pathol. **31**: 80–86. 2003. [Medline]
14. Wei M, Hori TA, Ichihara T, Wanibuchi H, Morimura K, Kang JS, Puatanachokchai R, and Fukushima S. Existence of no-observed effect levels for 2-amino-3,8-dimethylimidazo[4,5-f]quinoxaline on hepatic preneoplastic lesion development in BN rats. Cancer Lett. **231**: 304–308. 2006. [Medline] [CrossRef]
15. Fukushima S, Kinoshita A, Puatanachokchai R, Kushida M, Wanibuchi H, and Morimura K. Hormesis and dose-response-mediated mechanisms in carcinogenesis: evidence for a threshold in carcinogenicity of non-genotoxic carcinogens. Carcinogenesis. **26**: 1835–1845. 2005. [Medline] [CrossRef]
16. Wei M, Hamoud AS, Yamaguchi T, Kakehashi A, Morimura K, Doi K, Kushida M, Kitano M, Wanibuchi H, and Fukushima S. Potassium bromate enhances N-ethyl-N-hydroxyethylnitrosamine-induced kidney carcinogenesis only at high doses in Wistar rats: indication of the existence of an enhancement threshold. Toxicol Pathol. **37**: 983–991. 2009. [Medline] [CrossRef]
17. De Flora S. Threshold mechanisms and site specificity in chromium(VI) carcinogenesis. Carcinogenesis. **21**: 533–541. 2000. [Medline] [CrossRef]
18. Lutz WK, and Kopp-Schneider A. Threshold dose response for tumor induction by genotoxic carcinogens modeled via cell-cycle delay. Toxicol Sci. **49**: 110–115. 1999. [Medline] [CrossRef]
19. Kirsch-Volders M, Aardema M, and Elhajouji A. Concepts of threshold in mutagenesis and carcinogenesis. Mutat Res. **464**: 3–11. 2000. [Medline]
20. United States Environmental Protection Agency Supplementary Guidance for Conducting Health Risk Assessment of Chemical Mixtures (2000). http://cfpub.epa.gov/ncea/cfm/recordisplay.cfm?deid=20533.
21. Ruediger HW. Antagonistic combinations of occupational carcinogens. International Archives of Occupational and Environmental Health. **79**: 343–348. 2006. [Medline] [CrossRef]

Mutation Research 748 (2012) 29–35

Contents lists available at SciVerse ScienceDirect

Mutation Research/Genetic Toxicology and Environmental Mutagenesis

journal homepage: www.elsevier.com/locate/gentox
Community address: www.elsevier.com/locate/mutres

Dammar resin, a non-mutagen, inducts oxidative stress and metabolic enzymes in the liver of *gpt* delta transgenic mouse which is different from a mutagen, 2-amino-3-methylimidazo[4,5-*f*]quinoline

Xiao-Li Xie, Min Wei, Anna Kakehashi, Shotaro Yamano, Kyoko Okabe, Masaki Tajiri, Hideki Wanibuchi*

Department of Pathology, Osaka City University Graduate School of Medicine, Asahi-machi 1-4-3, Abeno-ku, 545-8585 Osaka, Japan

ARTICLE INFO

Article history:
Received 28 February 2012
Received in revised form 6 June 2012
Accepted 23 June 2012
Available online 6 July 2012

Keywords:
Dammar resin
IQ
Genotoxicity
Oxidative stress
Cytochrome P450s

ABSTRACT

Dammar resin has long been used in foods as either a clouding or a glazing agent. In a recent study, 2% Dammar resin showed significant hepatocarcinogenicity in a rat 2-year bioassay. Therefore, for an accurate estimate of human risk, it is necessary to understand whether Dammar resin induces liver genotoxicity and the underlying mechanisms of its hepatocarcinogenicity. Modifying effects of 2-amino-3-methylimidazo[4,5-*f*]quinoline (IQ), a typical genotoxic carcinogen produced during cooking of protein-rich foods, was also studied in the present study. Exposure of *gpt* delta mice to Dammar resin at a dose of 2% for 12 weeks did not induce any obvious mutagenicity in the liver. However, the index of cell proliferation, the level of 8-OHdG, and *bax*, *bcl-2*, *p53*, *cyp1a2*, *cyp2e1*, *gpx1* and *gstm2* gene expression were all significantly increased when compared with the control group. In the IQ treatment group, at a dose of 300 ppm, mutagenicity was readily detected, the index of cell proliferation increased, and *p53*, *cyp2e1* and *gpx1* gene expression was down-regulated in the liver. Down-regulation of *p53*, *P450s*, and *gpx1* in the livers of IQ treated mice are consistent with its genotoxic mechanism of carcinogenicity observed in a 675-day study. In contrast, our results using *gpt* delta mice suggest that Dammar resin is not genotoxic. Instead, the Dammar resin-induced hepatocarcinogenicity seen in our previous 2-year study with rats may have been mediated by non-genotoxic mechanisms, including increased P450 enzyme activity, increased oxidative stress, altered gene expression, and promotion of cell proliferation.

1. Introduction

Carcinogens can be classified into two categories, genotoxic and non-genotoxic. The former indicates a chemical capable of producing cancer by directly causing irreversible genetic damage, while the latter represents a chemical capable of producing cancer by some secondary mechanisms not related to direct gene damage [1].

Heterocyclic aromatic amines are the major class of genotoxic hepatocarcinogens in rodents [2]. 2-amino-3-methylimidazo[4,5-*f*]quinoline (IQ) is a genotoxic and carcinogenic heterocyclic amine formed by high-temperature cooking of proteinaceous food [2,3]. Long-term treatment (675 days) with 300 ppm IQ has been shown to induce tumors in the liver, lung and forestomach of CDF1 mice [4]. The In vivo mutagenicity and the mutation spectrum of IQ has been examined in commercially available transgenic rodent models such as BigBlue and guanine phosphoribosyltransferase (*gpt*) transgenic rats [3,5]. On the basis of these results, IQ was chosen as a positive mutagen for mutation assays.

Currently, little is known about Dammar resin metabolism. Dammar resin, isolated from plants belonging to the family Dipterocarpaceae, contains dammarane type triterpenes [6], which was reported to possess antiviral activities and to be protective against in vitro low density lipoprotein (LDL) oxidation [6,7]. Dammar resin is widely used in the food industry as a stabilizer and thickener. However, in a rat 2-year bioassay, the incidence of liver tumors was significantly increased in rats administered 2% Dammar resin when compared with the control group (unpublished data). The mechanism by which it exerts carcinogenic activity in rats has not been fully clarified.

The capability of a carcinogen to directly induce genetic mutations is routinely evaluated. However, in a recent study, up to 90% of rodent non-carcinogens tested positive in one or more of the standard in vitro assays used to determine the mutagenic capability of potential carcinogens, resulting in an unacceptably high number of false positive results [8]. Therefore, an in vivo genotoxicity test of Dammar resin and exploration of its mechanisms of hepatocarcinogenicity are required to help to evaluate the risk of this potential human carcinogen.

* Corresponding author. Tel.: +81 6 6645 3735; fax: +81 6 6646 3093.
E-mail address: wani@med.osaka-cu.ac.jp (H. Wanibuchi).

1383-5718/$ – see front matter © 2012 Elsevier B.V. All rights reserved.
http://dx.doi.org/10.1016/j.mrgentox.2012.06.005

8-hydroxydeoxyguanosine (8-OHdG) is well established as a representative biomarker for oxidative stress [9]: Oxidative damage to DNA is considered to be important in the mutagenesis and carcinogenesis process. The cytochrome P450s (P450s) act on a wide variety of chemicals, and their involvement in the production of reactive oxygen species during substrate oxidation is well documented [10,11]. Various chemicals with P450-inducible properties demonstrate hepatocarcinogenicity without overt genotoxicity [12–14], which suggests that reactive oxygen species resulting from increased activity of P450s enzymes may play a role in the carcinogenic activity of these chemicals. Researchers have hypothesized that non-genotoxic hepatocarcinogens with P450-inducible capability may cause oxidative damage to liver DNA, which might subsequently take part in inducing carcinogenesis [15].

The *gpt* delta mouse was established by microinjection of λ EG10 phage DNA (48 kb) into the fertilized eggs of C57BL/6J mice [16]. Progeny, carrying 80 copies of the transgene in a head-to-tail fashion at a single site of chromosome 17, were obtained and are maintained as homozygotes. These homozygous mice have been useful in the assessment of the in vivo genotoxicity and the estimation of carcinogenic risk of environmental chemicals [17].

In the present study, the in vivo genotoxicity of Dammar resin and IQ were examined using *gpt* delta mice and their possible mechanisms of hepatocarcinogenicity are discussed.

2. Materials and methods

2.1. Animals, diet and housing conditions

Eighteen male 5-week-old *gpt* delta C57BL/6J transgenic mice were obtained from Japan SLC and housed in plastic cages (six animals/cage) in our animal facility; animals were maintained under standard conditions (room temperature, 23 ± 1 °C; relative humidity, 44 ± 5%; and light/dark cycle, 12 h) and given free access to powdered diet (Oriental MF; Oriental Yeast, Tokyo, Japan) and tap water. Dammar resin was kindly provided by San-Ei Gen F.F.I., Inc., Osaka, Japan. The animals were acclimatized for 1 week prior to beginning the experiment. The experiment was conducted following approval of the Animal Care and Use Committee of the Osaka City University Graduate School of Medicine.

2.2. Animal treatments

Eighteen *gpt* delta transgenic mice were randomly divided into three groups (6 in each group) and were fed a basal diet or diet containing 2% Dammar resin or 300 part per million (ppm) of IQ for 12 weeks followed by 2-week basal diet, as described previously [18]. The dose levels of Dammar resin and IQ used in the present study are consistant with the carcinogenic levels which were studied in previous long-term carcinogenesis studies. In the present study, 12 weeks feeding with Dammar resin or IQ followed by a 2-week treatment-free period was employed because in previous transgenic studies using the *gpt* delta transgenic mouse [18,19], a positive response could be readily detected after a 12-week exposure to genotoxic carcinogens, and, in transgenic assays, it is important to choose an appropriate expression time, i.e., the time after the last exposure to mutagen which is required for the mutant frequency to stabilize in a given tissue [20]. An appropriate expression time for liver is 14 days [21].

All surviving animals were killed under deep anesthesia at the end of the experiment. The livers were isolated from each animal and immediately excised, weighted, and dissected into halves. One half was immediately frozen in liquid nitrogen and stored at −80 °C for mutation assays and gene expression analyses. The other half was cut into 2–3-mm thick slices. The slices were fixed in 10% buffered formalin solution and routinely processed to paraffin blocks for histopathological examination and immunohistochemistry. Hematoxylin and eosin (H&E)-stained tissue cut from the blocks were examined by light microscopy.

2.3. Immunohistochemistry staining for ki-67

Paraffin blocks of the livers were sectioned at 3-μm thickness. After deparaffinization, sections were incubated with 30% hydrogen peroxide to block endogenous peroxidase and antigen retrieval was performed by microwaving at 95 °C for 30 min. After blocking, sections were incubated with ki-67 primary antibody (1:500, 550690, BD Pharmingen, USA) overnight at 4 °C. Antigen visualization was done with 3,3′-diaminobenzidine tetrahydrochloride (DAB). To investigate proliferative activity, at least 1000 hepatocyte nuclei were counted in each liver; labeling indices were calculated as the percentage of cells positive for ki-67 staining.

2.4. Measurement of 8-OHdG

Nuclear DNA was extracted with a DNA Extractor WB kit (Wako Pure Chemical Industries) containing an antioxidant NaI solution to dissolve cellular components. For additional prevention of auto-oxidation in the cell lysis step, deferoxamine mesylate (Sigma Chemical, St Loius, MO, USA) was added to the lysis buffer. The DNA was digested into deoxynucleotides by treatment with nuclease P1 (Yamasa Shoyu, Chiba, Japan) and alkaline phosphatase (Sigma Chemical), and levels of 8-OHdG (8-OHdG/10^5 dG) were measured by high-performance liquid chromatography with an electrochemical detection system (Coulochem II; ESA, Bedford, MA, USA).

2.5. DNA isolation and in vitro packaging of λ phage DNA

High-molecular-weight genomic DNA was extracted from liver tissue using the RecoverEase DNA Isolation kit (Stratagene, La Jolla, CA, USA). λ EG10 phages were rescued using Transpack Packaging Extract (Stratagene).

2.6. gpt mutation assay

The assay was conducted according to previously published methods [16]. All the confirmed *gpt* mutants recovered from the livers were sequenced; identical mutations from the same mouse were counted as one mutant. The mutant frequency (MF) of the *gpt* gene in the liver was calculated by dividing the number of confirmed 6-thioguanine (6-TG)-resistant colonies by the number of rescued plasmids. DNA sequencing of the *gpt* gene was performed with the BigDye Terminater Cycle Sequencing Ready Reaction (Applied Biosystems, Inc., Carlsbad, CA, USA) on an Applied Biosystems PRISM 310 Genetic Analyzer.

2.7. Spi⁻ assay

The Spi⁻ assay was conducted according to previously published methods [16]. Packaged phages were incubated with *E. coli* XL-1 Blue MRA for survival titration and *E. coli* XL-1 Blue MRA P2 for mutant selection. Infected cells were mixed with molten lambda-trypticase agar plates. The next day, plaques (Spi⁻ candidates) were punched out with sterilized glass pipettes and the agar plugs were suspended in SM buffer. The Spi⁻ phenotype was confirmed by spotting the suspensions on three types of plates in which XL-1 Blue MRA, XL-1 Blue MRA P2, or WL95 P2 strains were spread with soft agar. True Spi⁻ mutants, which made clear plaques on all of the plates, were counted. Spi⁻ mutant lysates were obtained by infecting E. coli LE392with the recovered Spi⁻ mutants.

2.8. Quantitative real-time reverse transcription-polymerase chain reaction (RT-PCR) analysis of p53, bax, bcl-2, caspase-3, cyp1a1, cyp1a2, cyp2e1, cyp2r1, cyp7b1, glutathione peroxidase 1 (gpx1) and glutathion S-transferase mu 2 (gstm2) mRNA

Total RNA was extracted with TRIzol Reagent (Invitrogen) according to the manufacturer's instructions. cDNA copies of total RNA were obtained using a High Capacity cDNA Reverse Transcription kit (Applied Biosystems Japan Ltd.). Primers and probes (Taqman Gene Expression Assay) were purchased from Applied Biosystems, Inc., Carlsbad, CA, USA. The PCR program cycles were set as follows: initial denaturing at 95 °C for 20 s, followed by 40 cycles at 95 °C for 3 s, and 60 °C for 30 s. PCR reactions were performed as described previously [22], with primers for mouse *p53*, *bax*, *bcl-2*, *caspase-3*, *cyp1a1*, *cyp1a2*, *cyp2e1*, *cyp2r1*, *cyp7b1*, *gpx1* and *gstm2*. β-Actin mRNA was employed as an internal standard, and the mRNA levels of the target gene were normalized to the β-actin mRNA level. The Values in each treatment group were expressed as fold increases compared to the mean value in the control group, which was given an arbitrary value of 1.

2.9. Statistical analysis

All mean values were expressed as the mean ± standard deviation (SD). Statistical analyses were performed using the Statlight program (Yukms Co., Ltd., Tokyo, Japan). Homogeneity of variance was tested by the F test between the treatment and control groups. Differences in mean values between the treatment and control groups were evaluated by the two-tailed Student's *t*-test when variance was homogeneous and the two-tailed Aspin–Welch *t*-test when variance was heterogeneous. *p* values less than 0.05 were considered significant.

3. Results

3.1. Body and liver weights, water intake, food consumption and compound intake

The results for body and liver weights, water intake, food consumption and compound intake of the mice are presented in Table 1. In the Dammar resin group, one mouse died during the

Table 1
Final body weight, liver weight, water intake, food consumption and compounds intake of *gpt* delta transgenic mice.

Groups Number of effective mice	Control 6	2% Dammar resin 5	300 ppm IQ 6
Final body weight (g)	34.67 ± 1.87	28.76 ± 0.09*	30.7 ± 1.27*
Absolute liver weight (g)	1.20 ± 0.13	1.06 ± 0.08	1.38 ± 0.09*
Relative liver weight (g/g body weight)	0.035 ± 0.005	0.037 ± 0.003	0.045 ± 0.002*
Average water intake (g/g body weight/day)	0.24 ± 0.05	0.22 ± 0.03	0.26 ± 0.02
Average food intake (g/g body weight/day)	0.13 ± 0.02	0.12 ± 0.02	0.13 ± 0.02
Average compound intake (mg/g body weight/day)	–	2.43 ± 0.32	0.04 ± 0.01

* $p < 0.05$ versus the control group.

second week. Since the cause of death was unclear, it was not included in the final analysis.

Dammar resin and IQ did not affect average water or food intake, but significantly suppressed final body weight. No significant changes of absolute or relative liver weights were observed in the Dammar resin-treated group. The absolute and relative liver weights were significantly increased in the IQ-treated group ($p < 0.05$).

3.2. Histopathological evaluation and hepatocyte proliferation analysis

There were no obvious pathologic changes in the livers of the Dammar resin group; hypertrophy and vacuolar degeneration of hepatocytes were observed in some livers of IQ-treated mice (data not shown).

Fig. 1 shows the results of cell proliferation analysis by ki-67 staining. Proliferation of hepatocytes was significantly elevated in both Dammar resin and IQ treatment groups compared with the control group.

3.3. Examination of oxidative stress by 8-OHdG measurement

Fig. 2 shows the 8-OHdG levels in the livers. Significant increases of 8-OHdG were present in the Dammar resin-treated group, but not in the IQ treatment group, compared with the control group.

3.4. In vivo mutation assay

Data for *gpt* MF analyzed by 6-TG selection are summarized in Table 2. There was no difference in the *gpt* MF in the Dammar resin-treated mice (3.01×10^{-6}) compared with the control group (5.39×10^{-6}). In contrast, in the IQ-treated mice, *gpt* MF (32.49×10^{-6}) was significantly increased, approximately 6-fold higher than the control group.

To characterize the *gpt* mutations in the livers, DNA sequencing was performed (Table 3). In Dammar resin-treated mice, the predominant types of base substitutions were G:C to A:T transitions (5/12 = 41.7%) and G:C to T:A transversions (3/12 = 25%), neither of which differed significantly from the control group. On the other hand, the predominant type of base substitution in the IQ treatment group was the G:C to T:A transversion (81/117 = 69.2%), which was significantly increased compared to the control group.

The results of the Spi$^-$ mutation assay are shown in Table 4. There was no difference in Spi$^-$ mutant frequency in the mice administered Dammar resin (5.94 ± 3.00, $p > 0.05$), but Spi$^-$ mutant frequency in mice fed IQ (21.69 ± 10.44, $p < 0.01$) is significantly elevated compared to the control (6.21 ± 1.05).

3.5. mRNA expression levels of p53, bax, bcl-2, caspase-3, cyp1a1, cyp1a2, cyp2e1, cyp2r1, cyp7b1, gpx1 and gstm2 in mouse liver

RT-PCR was performed on all the mice livers. The results are shown in Fig. 3. Expression of *p53*, *bax*, *bcl-2*, *cyp1a2*, *cyp2e1*, *gpx1* and *gstm2* were significantly increased in Dammar resin-treated mice ($p < 0.05$). Expression of *p53*, *cyp2e1* as well as *gpx1* were

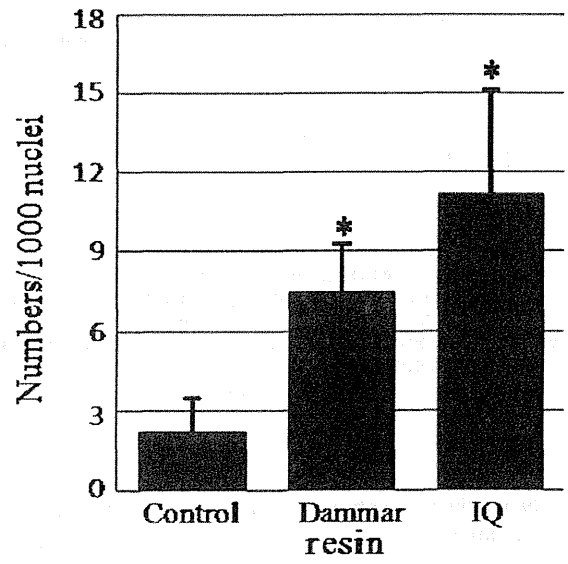

Fig. 1. Cell proliferation index. Compared with the control group, hepatocyte proliferation was significantly elevated by administeration of Dammar resin or IQ, at doses of 2% and 300 ppm, respectively. Significant compared with the control group (*$p < 0.05$).

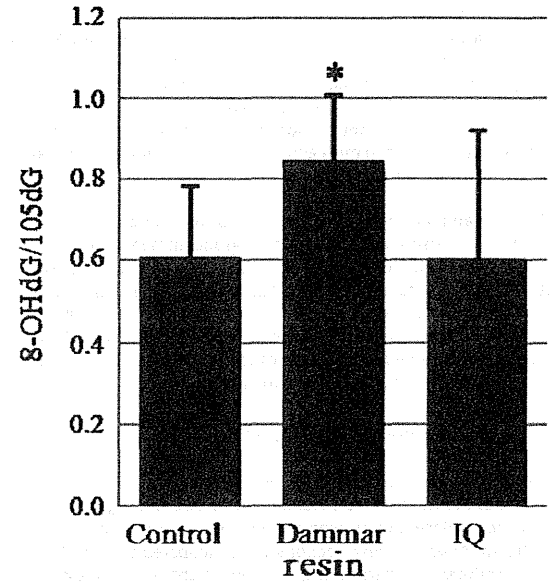

Fig. 2. Formation of 8-OHdG in the liver. The level of 8-OHdG was significantly increased by treatment with 2% Dammar resin, while no change was observed with 300 ppm IQ treatment. Significant compared with the control group (*$p < 0.05$).

Table 2
gpt mutation frequency in mouse livers.

Treatment	Mouse number	Cm^R colonies ($\times 10^5$)	Independent *gpt* mutation	*gpt* MF ($\times 10^{-6}$)	Mean ± SD
Control	11	7.80	3	3.85	5.39 ± 2.78
	12	7.08	4	5.65	
	13	7.29	3	4.12	
	14	6.27	6	9.57	
	15	5.64	1	1.77	
	16	5.40	4	7.41	
2% Dammar resin	21	9.60	2	2.08	3.01 ± 1.19
	22	5.52	1	1.81	
	23	7.48	2	2.67	
	24	5.10	2	3.92	
	26	10.96	5	4.56	
300 ppm IQ	31	6.51	14	21.51	32.49 ± 11.14*
	32	5.13	19	37.04	
	33	6.99	22	31.47	
	34	6.99	17	24.32	
	35	6.36	18	28.30	
	36	5.16	27	52.33	

* $p < 0.01$ versus the control group.

Table 3
Classification of *gpt* mutations in *gpt* delta mouse livers.

Types of *gpt* mutation	Control		2% Dammar resin		300 ppm IQ	
	Number (%)	Mutant frequency ($\times 10^{-6}$)	Number (%)	Mutant frequency ($\times 10^{-6}$)	Number (%)	Mutant frequency ($\times 10^{-6}$)
Base substitution						
Transition						
G:C to A:T	3(14.3)	0.71 ± 0.79	5(41.7)	1.18 ± 1.19	8(6.8)	2.25 ± 1.80
A:T to G:C	2(9.5)	0.49 ± 0.77	1(8.3)	0.39 ± 0.88	3(2.6)	0.76 ± 1.30
Transversion						
G:C to T:A	5(23.8)	1.25 ± 1.07	3(25)	0.68 ± 0.97	81(69.2)	22.56 ± 7.17*
G:C to C:G	1(4.8)	0.24 ± 0.58	0	0 ± 0	7(6)	1.92 ± 2.53
A:T to T:A	0	0 ± 0	0	0 ± 0	2(1.7)	0.65 ± 1.59
A:T to C:G	2(9.5)	0.57 ± 0.89	0	0 ± 0	1(0.9)	0.26 ± 0.64
Deletion						
Single bp	2(9.5)	0.45 ± 0.70	0	0 ± 0	6(5.1)	1.65 ± 1.83
Over 2bp	1(4.8)	0.31 ± 0.76	0	0 ± 0	2(1.7)	0.49 ± 0.77
Insertion	5(23.8)	1.36 ± 1.70	2(16.7)	0.57 ± 0.87	6(5.1)	1.63 ± 1.59
Others	0	0 ± 0	1(8.3)	0.18 ± 0.41	1(0.9)	0.32 ± 0.79
Total	21 (100)	5.39 ± 2.78	12 (100)	3.01 ± 1.19	117 (100)	32.49 ± 11.14*

* $p < 0.01$ versus the control group.

significantly decreased in IQ-treated mice ($p < 0.05$). The ratio of *bax* versus *bcl-2* as well as expression of *caspase-3*, *cyp1a1*, *cyp2r1* and *cyp7b1* did not differ in the treated groups compared with the control group.

4. Discussion

IQ is known to be a potent mutagen for the liver [23], and it was therefore used as a positive control mutagen for validating

Table 4
Spi^- mutant frequency in mouse livers.

Treatment	Mouse number	Plaques within XL-1 Blue MRA ($\times 10^5$)	Plaque within WL95 (P2)	Mutant frequency ($\times 10^{-6}$)	Mean ± SD
Control	11	13.06	6	4.59	6.21 ± 1.05
	12	10.22	7	6.85	
	13	11.24	7	6.23	
	14	10.58	8	7.56	
	15	10.92	6	5.49	
	16	24.39	16	6.56	
2% Dammar resin	21	15.96	4	2.51	5.94 ± 3.00
	22	13.72	13	9.48	
	23	14.44	6	4.16	
	24	10.38	9	8.67	
	26	10.18	5	4.91	
300 ppm IQ	31	10.16	15	14.76	21.69 ± 10.44*
	32	12.24	20	16.34	
	33	14.26	49	34.36	
	34	14.12	29	20.54	
	35	21.68	21	9.69	
	36	11.04	38	34.42	

* $p < 0.01$ versus the control group.

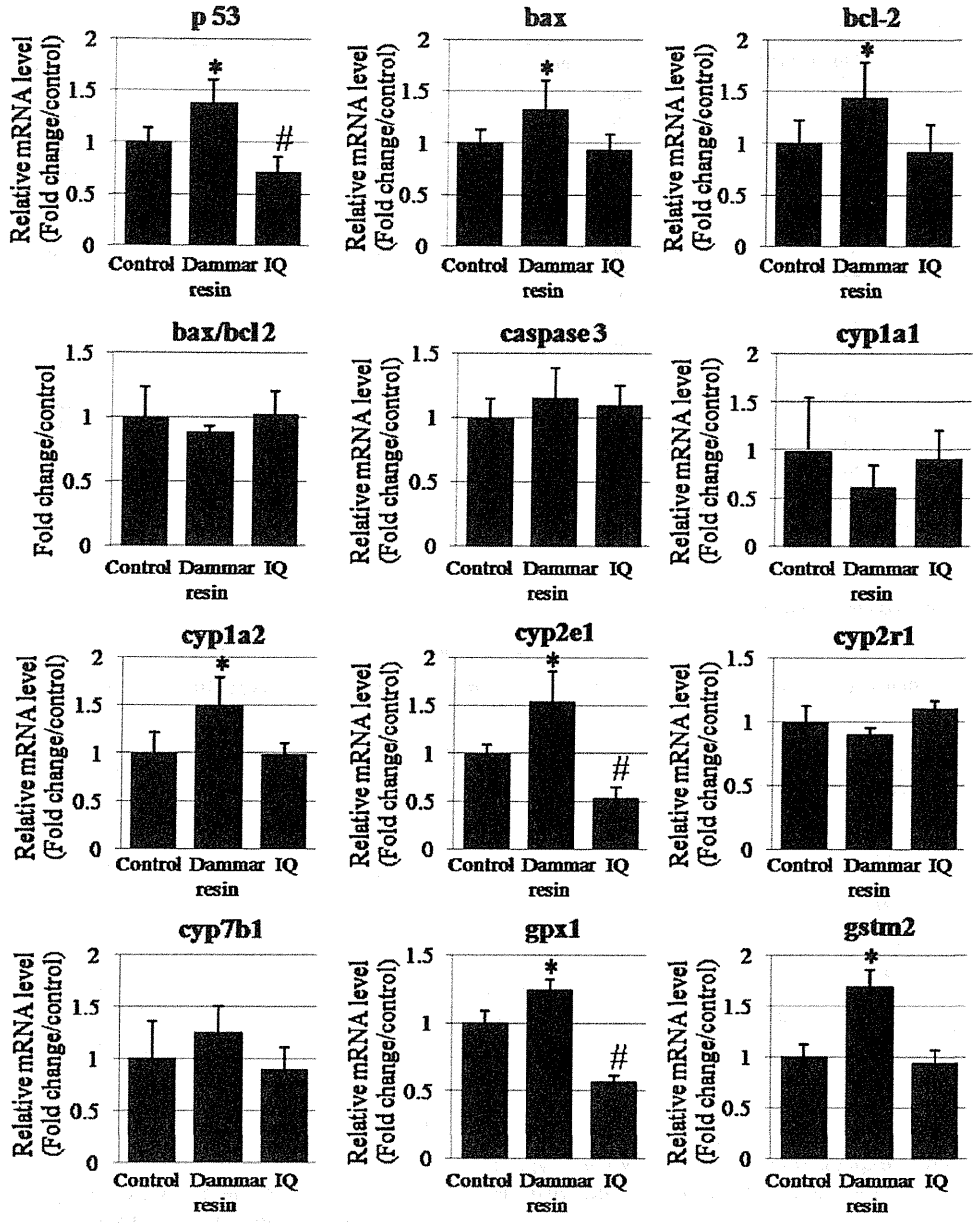

Fig. 3. mRNA expression of *p53*, *bax*, *bcl-2*, *bax/bcl-2*, *caspase-3*, *cyp1a1*, *cyp1a2*, *cyp2e1*, *cyp2r1*, *cyp7b1*, *gpx1* and *gstm2* in the livers of *gpt* delta mice. Significantly increased *p53*, *bax*, *bcl-2*, *cyp1a2*, *cyp2e1*, *gpx1* and *gstm2* gene expression was observed in the Dammar resin-treated group, while significantly decreased *p53*, *cyp2e1* and *gpx1* gene expression was observed in the IQ-administered group. The ratio of *bax* versus *bcl-2* as well as the mRNA expression of *caspase-3*, *cyp1a1*, *cyp2r1* and *cyp7b1* did not differ in the treated and control groups. Significantly up-regulated compared with the control group ($^{*}p < 0.05$); significantly down-regulated compared with the control group ($^{\#}p < 0.05$).

the mutagenicity assay system. In the present study, the mutation assay clearly showed that exposure to IQ at a dose of 300 ppm for 12 weeks was mutagenic. Significant increases in *gpt* MF, for the detection of point mutations, and Spi$^-$ MF, mainly attributable to deletion mutations, were found in IQ-treated mice. In the *gpt* assay, IQ primarily caused transversion of G:C to T:A, which is consistent with previous studies [3,5].

On the other hand, exposure to Dammar resin at a dose of 2% for 12 weeks was not mutagenic, which was consistent with the results of our mutation assay conducted in *gpt* delta transgenic rats (manuscript in preparation). There was no change in either the *gpt* MF or Spi$^-$ MF between the Dammar resin and control group. In the Dammar resin-administered group, the predominant types of base substitutions were G:C to A:T transitions and G:C to T:A transversions, neither of which were significantly different from the control group.

Ki-67 is a nuclear marker of cell proliferation and is detectable in the cell at all phases of the cell cycle except G_0 [24]. The ki-67 labeling index is associated with liver cancer outcome [25]. In the present study, proliferation of hepatocytes was significantly augmented by administration of both IQ and Dammar resin, suggesting the possibility that enhanced cell proliferation might be at least partly responsible for the carcinogenic activity of these agents.

Oxidative DNA damage with 8-OHdG formation is reported to be induced by 2-amino-imidazo[4,5-*f*]quinoline [23] and is thought to play a critical role in IQ-mediated carcinogenesis. However, in the present study, IQ did not induce 8-OHdG formation. Our result was consistent with the studies of Kitamura et al. [26] and Wei et al. [22]: the level of 8-OHdG was not significantly changed in the livers of rats treated with 300 ppm IQ.

It is generally recognized that oxidative stress occurs in a cell or tissue when the concentration of reactive oxygen species (ROS)

generated exceeds the antioxidant capability of that cell [27]. ROS generation is related to P450 enzyme activity. Multiple sources of ROS may contribute to persistent oxidative stress, resulting in higher 8-OHdG levels, and subsequently resulting in pathophysiologic changes that allow for the selective growth of preneoplastic initiated cells [27]. In the present study, levels of P450 enzymes and 8-OHdG levels were increased in the Dammar resin fed group, suggesting that Dammar resin may induce the expression and activity of P450 enzymes which would result in increased ROS production and 8-OHdG generation. However, while the Dammar resin fed group had increased 8-OHdG levels, there was no evidence suggestive of direct DNA damage, i.e., the Dammar resin fed group did not have increased DNA mutations. Therefore, our results suggest that the production of reactive oxygen species resulting from increased expression and activity of P450 enzymes, while causing chemical damage to DNA bases, is insufficient to cause permanent gene mutations; this result is consistent with a previous study [15].

Disruption of apoptosis can promote tumor initiation and progression [28], and the induction of apoptosis is central to the tumor-suppressive activity of p53 [29]. Bax is a proapoptotic Bcl-2 family member that binds to the anti-apoptotic Bcl-2 protein and antagonizes its function [30]. The *bax* gene is known to be transcriptionally regulated by p53 during induction of apoptosis [31,32]. Thus, up-regulated *bax* is one mechanism whereby p53 induces apoptosis [33]. Furthermore, p53 loss and Bcl-2 overexpression can have virtually identical effects on the pathology of some tumors [34]. Caspase-3 is a key mediator of apoptosis and can be activated through both extrinsic and intrinsic signaling pathways [35,36]. In the present study, treatment with IQ significantly down-regulated expression of *p53* expression, but did not affect expression of *bax*, *bcl-2* or *caspase-3* or change the ratio of *bax* versus *bcl-2*. Treatment with Dammar resin significantly increased expression of *p53*, *bax* and *bcl-2* genes, but did not change the ratio of *bax* versus *bcl-2* or change expression of *caspase-3*. This suggests that neither IQ nor Dammar resin affected basal apoptotic/anti-apoptotic signaling in hepatocytes, but expression of *p53*, the upstream inhibitor of *bcl-2* and activator of apoptosis [34], was affected by these agents: IQ suppressed expression of *p53* mRNA while Dammar resin induced expression of *p53* mRNA. This suggests that in the livers of *gpt* delta mice, the genotoxic agent IQ suppresses apoptotic removal of mutated cells with carcinogenic potential while the non-genotoxic agent Dammar resin does not suppress apoptotic removal of cells with carcinogenic potential. This also explains why Dammar resin increased the formation of 8-OHdG but did not cause an increase in mutation frequency in the livers of Dammar resin treated mice.

P450s are the predominant catalysts of phase I metabolism in the liver. It has been generally accepted that the various forms of P450s show different rates of activation as well as detoxication of chemical carcinogens [37]. Gpx1 is a phase II enzyme: Gpx1 is one of the most important of the antioxidant phase II metabolic enzymes which protect cells and tissues from damage caused by reactive oxygen species by helping to maintain the balance between prooxidant and antioxidant forces [38]. Gstm2 is another phase II enzyme: Gstm2 is a member of the Glutathione S-transferase (GST) family which represents a major group of detoxification enzymes [39].

In our study, mRNA levels of *cyp2e1* were significantly down-regulated by treatment with IQ. In addition, IQ itself is able to affect the activity of P450s enzymes depending on the treatment regimen [40]. Low P450s enzyme activity would delay the metabolic conversion of IQ into a substrate for GST enzymes and this may be one factor in the low mRNA levels of *gpx1* after treatment with IQ. Morgan et al. [41] suggest that low levels of P450s mRNA and proteins in tumor-bearing mice and repression of hepatic transport proteins is linked with reduced drug clearance and the resultant toxicity of the drug. Taken together, these data suggest that the delay of metabolic transformation of IQ and its metabolites may be involved in its toxicity.

In the Dammar resin treatment group, mRNA levels of *cyp1a2*, *cyp2e1*, *gpx1* and *gstm2* were significantly up-regulated compared to the control group. While induction of detoxification and antioxidant enzymes (*gpx1* and *gstm2*) is protective [41,42], induction of these enzymes also indicates production of reactive metabolites by phase I enzymes. Importantly, induction of P450s by chemicals can induce hepatocarcinogenicity in rodents without overt genotoxicity [13,14]. Induction of P450s (*cyp1a2* and *cyp2e1*) by Dammar resin administration might play a role in carcinogenicity through mechanisms related to oxidative stress [43]: Klaunig et al. [27] have shown that chronic sublethal oxidative injury can alter cellular metabolic pathways and gene expression, leading to altered cell growth in the absence of genetic mutations. Thus, we hypothesize that intranuclear oxidative stress could play a role in Dammar resin hepatocarcinogenicity by altering gene expression as a result of 8-OHdG adduct formation, but not by inducing DNA mutation. Therefore, consistent with a previous study by Tasaki et al. [15], it is reasonable to suggest that the hepatocarcinogenicity of Dammar resin observed in our previous long-term experiment with rats (unpublished data) may not be caused by DNA mutations, but rather by non-genotoxic mechanisms: Promotion of cell proliferation, induction of P450s, detoxification and antioxidant enzymes, increased intranuclear oxidative stress and other gene products. Although the mechanisms responsible for the carcinogenicity of Dammar resin remain to be further defined, our findings support the suggestion that its carcinogenicity does not necessarily correlate with in vivo mutagenicity [1].

In a recent study, 20 terpenoids from Dammar resin are pointed to have cytotoxic activity against human leukemia (HL60) and melanoma (RL1579) cells in vitro, which suggest that triterpenoids isolated from Dammar resin and its derivatives are valuable as potential cancer chemopreventive agents [7]. However, although no genetoxicity was observed in Dammar resin-treated group in the present study, considering its hepatocarcinogenesis in rats, Dammar resin should be used with care, if used at all, as a cancer chemopreventive agent until further investigations are conducted focusing on its metabolism and the underlying mechanisms of its hepatocarcinogenicity. Furthermore, the results of the present study suggest that Dammar resin has potential carcinogenic activity in mice.

In summay, administration of the known genotoxic hepatocarcinogen IQ results in increased liver cell proliferation and a characteristic mutation spectra with a predominant occurrence of G:C to T:A transitions in the *gpt* sequence analysis. Decreased expression of *cyp2e1* and *gpx1* increases the genotoxicity of IQ and decreased expression of p53 allows the survival and proliferation of cells with mutated DNA, suggesting that the hepatocarcinogenicity of IQ is initiated by DNA mutation. Like IQ, administration of Dammar resin to *gpt* delta mice also promotes liver cell proliferation; however, unlike IQ, Dammar resin administration does not cause DNA mutation. Rather, Dammar resin promotes cell proliferation, induces expression metabolic enzymes, and increases intranuclear oxidative stress. These results suggest that Dammar resin is a potential hepatocarcinogen in mice, although this remains to be verified. Dammar resin does not increase DNA mutation frequency, indicating that it is non-genotoxic in mice, which is consistent with our results of mutation assay conducted in *gpt* delta rats (manuscript in preparation). Importantly, the possible mechanism of Dammar resin-mediated carcinogenicity suggested by the results of the present study is also active in humans, indicating that the use of Dammar resin or its constituents in foods or as a food supplement for humans should be carefully monitored.

Conflict of interest statement

The authors declare that there are no conflicts of interest.

Acknowledgements

This work was partly supported by a Grant-in-Aid for Scientific Research from the Ministry of Health, Labor and Welfare of Japan. We thank Yumi Obo and Rie Onodera for their technical assistance and Yukiko Iura for her help during preparation of this manuscript.

References

[1] Y. Hayashi, Overview of genotoxic carcinogens and non-genotoxic carcinogens, Exp. Toxicol. Pathol. 44 (1992) 465–471.
[2] K. Wakabayashi, M. Nagao, H. Esumi, T. Sugimura, Food-derived mutagens and carcinogens, Cancer Res. 52 (1992) 2092s–2098s.
[3] K. Kanki, A. Nishikawa, K. Masumura, T. Umemura, T. Imazawa, Y. Kitamura, T. Nohmi, M. Hirose, In vivo mutational analysis of liver DNA in gpt delta transgenic rats treated with the hepatocarcinogens N-nitrosopyrrolidine, 2-amino-3-methylimidazo[4,5-*f*]quinoline, and di(2-ethylhexyl)phthalate, Mol. Carcinogen. 42 (2005) 9–17.
[4] H. Ohgaki, K. Kusama, N. Matsukura, K. Morino, H. Hasegawa, S. Sato, S. Takayama, T. Sugimura, Carcinogenicity in mice of a mutagenic compound, 2-amino-3-methylimidazo[4,5-*f*]quinoline, from broiled sardine, cooked beef and beef extract, Carcinogenesis 5 (1984) 921–924.
[5] S.A. Bol, J. Horlbeck, J. Markovic, J.G. de Boer, R.J. Turesky, A. Constable, Mutational analysis of the liver, colon and kidney of Big Blue rats treated with 2-amino-3-methylimidazo[4,5-*f*]quinoline, Carcinogenesis 21 (2000) 1–6.
[6] B.L. Poehland, B.K. Carte, T.A. Francis, L.J. Hyland, H.S. Allaudeen, N. Troupe, In vitro antiviral activity of dammar resin triterpenoids, J. Nat. Prod. 50 (1987) 706–713.
[7] M. Ukiya, T. Kikuchi, H. Tokuda, K. Tabata, Y. Kimura, T. Arai, Y. Ezaki, O. Oseto, T. Suzuki, T. Akihisa, Antitumor-promoting effects and cytotoxic activities of dammar resin triterpenoids and their derivatives, Chem. Biodivers. 7 (2010) 1871–1884.
[8] D. Kirkland, M. Aardema, L. Henderson, L. Muller, Evaluation of the ability of a battery of three in vitro genotoxicity tests to discriminate rodent carcinogens and non-carcinogens. I. Sensitivity, specificity and relative predictivity, Mutat. Res. 584 (2005) 1–256.
[9] A. Kinoshita, H. Wanibuchi, S. Imaoka, M. Ogawa, C. Masuda, K. Morimura, Y. Funae, S. Fukushima, Formation of 8-hydroxydeoxyguanosine and cell-cycle arrest in the rat liver via generation of oxidative stress by phenobarbital: association with expression profiles of p21(WAF1/Cip1), cyclin D1 and Ogg1, Carcinogenesis 23 (2002) 341–349.
[10] A. Sapone, B. Gustavino, M. Monfrinotti, D. Canistro, M. Broccoli, L. Pozzetti, A. Affatato, L. Valgimigli, G.C. Forti, G.F. Pedulli, G.L. Biagi, S.Z. Abdel-Rahman, M. Paolini, Perturbation of cytochrome P450, generation of oxidative stress and induction of DNA damage in Cyprinus carpio exposed in situ to potable surface water, Mutat. Res. 626 (2007) 143–154.
[11] K.D. Nichols, G.M. Kirby, Expression of cytochrome P450 2A5 in a glucose-6-phosphate dehydrogenase-deficient mouse model of oxidative stress, Biochem. Pharmacol. 75 (2008) 1230–1239.
[12] Y. Dewa, J. Nishimura, M. Muguruma, M. Jin, Y. Saegusa, T. Okamura, M. Tasaki, T. Umemura, K. Mitsumori, beta-Naphthoflavone enhances oxidative stress responses and the induction of preneoplastic lesions in a diethylnitrosamine-initiated hepatocarcinogenesis model in partially hepatectomized rats, Toxicology 244 (2008) 179–189.
[13] Y. Dewa, J. Nishimura, M. Muguruma, M. Jin, M. Kawai, Y. Saegusa, T. Okamura, T. Umemura, K. Mitsumori, Involvement of oxidative stress in hepatocellular tumor-promoting activity of oxfendazole in rats, Arch. Toxicol. 83 (2009) 503–511.
[14] M. Kawai, Y. Saegusa, Y. Dewa, J. Nishimura, S. Kemmochi, T. Harada, Y. Ishii, T. Umemura, M. Shibutani, K. Mitsumori, Elevation of cell proliferation via generation of reactive oxygen species by piperonyl butoxide contributes to its liver tumor-promoting effects in mice, Arch. Toxicol. 84 (2010) 155–164.
[15] M. Tasaki, T. Umemura, Y. Suzuki, D. Hibi, T. Inoue, T. Okamura, Y. Ishii, S. Maruyama, T. Nohmi, A. Nishikawa, Oxidative DNA damage and reporter gene mutation in the livers of gpt delta rats given non-genotoxic hepatocarcinogens with cytochrome P450-inducible potency, Cancer Sci. 101 (2010) 2525–2530.
[16] T. Nohmi, M. Katoh, H. Suzuki, M. Matsui, M. Yamada, M. Watanabe, M. Suzuki, N. Horiya, O. Ueda, T. Shibuya, H. Ikeda, T. Sofuni, A new transgenic mouse mutagenesis test system using Spi- and 6-thioguanine selections, Environ. Mol. Mutagen. 28 (1996) 465–470.
[17] K. Masumura, M. Matsui, M. Katoh, N. Horiya, O. Ueda, H. Tanabe, M. Yamada, H. Suzuki, T. Sofuni, T. Nohmi, Spectra of gpt mutations in ethylnitrosourea-treated and untreated transgenic mice, Environ. Mol. Mutagen. 34 (1999) 1–8.
[18] K. Masumura, Y. Totsuka, K. Wakabayashi, T. Nohmi, Potent genotoxicity of aminophenylnorharman, formed from non-mutagenic norharman and aniline, in the liver of gpt delta transgenic mouse, Carcinogenesis 24 (2003) 1985–1993.
[19] T. Suzuki, M. Hayashi, M. Ochiai, K. Wakabayashi, T. Ushijima, T. Sugimura, M. Nagao, T. Sofuni, Organ variation in the mutagenicity of MeIQ in Big Blue lacI transgenic mice, Mutat. Res. 369 (1996) 45–49.
[20] J.A. Heddle, P. Shaver-Walker, K.S. Tao, X.B. Zhang, Treatment protocols for transgenic mutation assays in vivo, Mutagenesis 10 (1995) 467–470.
[21] T. Suzuki, S. Itoh, M. Nakajima, N. Hachiya, T. Hara, Target organ and time-course in the mutagenicity of five carcinogens in MutaMouse: a summary report of the second collaborative study of the transgenic mouse mutation assay by JEMS/MMS, Mutat. Res. 444 (1999) 259–268.
[22] M. Wei, H. Wanibuchi, D. Nakae, H. Tsuda, S. Takahashi, M. Hirose, Y. Totsuka, M. Tatematsu, S. Fukushima, Low-dose carcinogenicity of 2-amino-3-methylimidazo[4,5-*f*]quinoline in rats: evidence for the existence of no-effect levels and a mechanism involving p21(Cip/WAF1), Cancer Sci. 102 (2011) 88–94.
[23] V.M. Lakshmi, F.F. Hsu, T.V. Zenser, N-Demethylation is a major route of 2-amino-3-methylimidazo[4,5-*f*]quinoline metabolism in mouse, Drug Metab. Dispos. 36 (2008) 1143–1152.
[24] J. Gerdes, U. Schwab, H. Lemke, H. Stein, Production of a mouse monoclonal antibody reactive with a human nuclear antigen associated with cell proliferation, Int. J. Cancer 31 (1983) 13–20.
[25] M. Nolte, M. Werner, A. Nasarek, H. Bektas, R. von Wasielewski, J. Klempnauer, A. Georgii, Expression of proliferation associated antigens and detection of numerical chromosome aberrations in primary human liver tumours: relevance to tumour characteristics and prognosis, J. Clin. Pathol. 51 (1998) 47–51.
[26] Y. Kitamura, T. Umemura, K. Okazaki, K. Kanki, T. Imazawa, T. Masegi, A. Nishikawa, M. Hirose, Enhancing effects of simultaneous treatment with sodium nitrite on 2-amino-3-methylimidazo[4,5-*f*]quinoline-induced rat liver, colon and Zymbal's gland carcinogenesis after initiation with diethylnitrosamine and 1,2-dimethylhydrazine, Int. J. Cancer 118 (2006) 2399–2404.
[27] J.E. Klaunig, Y. Xu, J.S. Isenberg, S. Bachowski, K.L. Kolaja, J. Jiang, D.E. Stevenson, E.F. Walborg Jr., The role of oxidative stress in chemical carcinogenesis, Environ. Health Perspect. 106 (Suppl. 1) (1998) 289–295.
[28] S.W. Lowe, A.W. Lin, Apoptosis in cancer, Carcinogenesis 21 (2000) 485–495.
[29] C.A. Schmitt, J.S. Fridman, M. Yang, E. Baranov, R.M. Hoffman, S.W. Lowe, Dissecting p53 tumor suppressor functions in vivo, Cancer Cell 1 (2002) 289–298.
[30] Z.N. Oltvai, C.L. Milliman, S.J. Korsmeyer, Bcl-2 heterodimerizes in vivo with a conserved homolog, Bax, that accelerates programmed cell death, Cell 74 (1993) 609–619.
[31] L. Buckbinder, R. Talbott, S. Velasco-Miguel, I. Takenaka, B. Faha, B.R. Seizinger, N. Kley, Induction of the growth inhibitor IGF-binding protein 3 by p53, Nature 377 (1995) 646–649.
[32] T. Miyashita, J.C. Reed, Tumor suppressor p53 is a direct transcriptional activator of the human bax gene, Cell 80 (1995) 293–299.
[33] A. Thomas, T. Giesler, E. White, p53 mediates bcl-2 phosphorylation and apoptosis via activation of the Cdc42/JNK1 pathway, Oncogene 19 (2000) 5259–5269.
[34] M.T. Hemann, S.W. Lowe, The p53-Bcl-2 connection, Cell Death Differ. 13 (2006) 1256–1259.
[35] S. Kothakota, T. Azuma, C. Reinhard, A. Klippel, J. Tang, K. Chu, T.J. McGarry, M.W. Kirschner, K. Koths, D.J. Kwiatkowski, L.T. Williams, Caspase-3-generated fragment of gelsolin: effector of morphological change in apoptosis, Science 278 (1997) 294–298.
[36] S. Ghavami, M. Hashemi, S.R. Ande, B. Yeganeh, W. Xiao, M. Eshraghi, C.J. Bus, K. Kadkhoda, E. Wiechec, A.J. Halayko, M. Los, Apoptosis and cancer: mutations within caspase genes, J. Med. Genet. 46 (2009) 497–510.
[37] A.H. Conney, Induction of microsomal enzymes by foreign chemicals and carcinogenesis by polycyclic aromatic hydrocarbons: G.H.A. Clowes Memorial Lecture, Cancer Res. 42 (1982) 4875–4917.
[38] X. Chen, T.O. Scholl, M.J. Leskiw, M.R. Donaldson, T.P. Stein, Association of glutathione peroxidase activity with insulin resistance and dietary fat intake during normal pregnancy, J. Clin. Endocrinol. Metab. 88 (2003) 5963–5968.
[39] J.D. Hayes, D.J. Pulford, The glutathione S-transferase supergene family: regulation of GST and the contribution of the isoenzymes to cancer chemoprotection and drug resistance, Crit. Rev. Biochem. Mol. Biol. 30 (1995) 445–600.
[40] R.A. McPherson, M.D. Tingle, L.R. Ferguson, Contrasting effects of acute and chronic dietary exposure to 2-amino-3-methyl-imidazo[4,5-*f*]quinoline (IQ) on xenobiotic metabolising enzymes in the male Fischer 344 rat: implications for chemoprevention studies, Eur. J. Nutr. 40 (2001) 39–47.
[41] E.T. Morgan, K.B. Goralski, M. Piquette-Miller, K.W. Renton, G.R. Robertson, M.R. Chaluvadi, K.A. Charles, S.J. Clarke, M. Kacevska, C. Liddle, T.A. Richardson, R. Sharma, C.J. Sinal, Regulation of drug-metabolizing enzymes and transporters in infection, inflammation, and cancer, Drug Metab. Dispos. 36 (2008) 205–216.
[42] K. Shimamoto, Y. Dewa, Y. Ishii, S. Kemmochi, E. Taniai, H. Hayashi, M. Imaoka, R. Morita, K. Kuwata, K. Suzuki, M. Shibutani, K. Mitsumori, Indole-3-carbinol enhances oxidative stress responses resulting in the induction of preneoplastic liver cell lesions in partially hepatectomized rats initiated with diethylnitrosamine, Toxicology 283 (2011) 109–117.
[43] Y. Minamiyama, S. Takemura, S. Toyokuni, S. Imaoka, Y. Funae, K. Hirohashi, T. Yoshikawa, S. Okada, CYP3A induction aggravates endotoxemic liver injury via reactive oxygen species in male rats, Free Radic. Biol. Med. 37 (2004) 703–712.

MUC5AC protects pancreatic cancer cells from TRAIL-induced death pathways

HIROTAKA HOSHI[1,3], TETSUJI SAWADA[2], MOTOYUKI UCHIDA[1], HIROKO IIJIMA[1], KENJIRO KIMURA[2], KOSEI HIRAKAWA[2] and HIDEKI WANIBUCHI[3]

[1]Biomedical Research Laboratories, Kureha Corporation, Shinjuku-ku, Tokyo 169-8503; Departments of [2]Surgical Oncology and [3]Pathology, Osaka City University Graduate School of Medicine, Abeno-ku, Osaka 545-8585, Japan

Received September 3, 2012; Accepted November 12, 2012

DOI: 10.3892/ijo.2013.1760

Abstract. We have previously reported that a specific siRNA transfected MUC5AC could knockdown MUC5AC expression and suppress *in vivo* tumor growth and metastasis, although it had no effects on *in vitro* cell growth, cell survival, proliferation and morphology. In the present study, we investigated which host immune cells induced these effects and how the effects were induced using immunocyte-depleted animal models. The tumor growth of SW1990/si-MUC5AC cells, which show no tumor growth when implanted subcutaneously into a nude mouse, was recovered when neutrophils were removed by anti-Gr-1 mAb administration. This result suggests that MUC5AC may suppress the antitumor effects of neutrophils by allowing tumor cells to escape the host immune system. Subsequently, we investigated the effects of MUC5AC on apoptosis induction mediated by TNF-related apoptosis-inducing ligand (TRAIL), one of the antitumor mechanisms of neutrophils. SW1990/si-MUC5AC cells showed significantly increased active caspase 3 expression after the addition of TRAIL. On the other hand, SW1990/si-mock cells showed no such changes. Our results indicate that MUC5AC inhibits TRAIL-induced apoptosis in human pancreatic cancer and may serve as an important indicator in diagnosis and prognosis.

Introduction

Pancreatic cancer is the 8th and 9th leading cause of cancer-related deaths worldwide in men and women. More than 50% of patients are diagnosed with advanced disease and have metastatic disease at presentation, 10 to 15% will be resectable, and the remainder will be locally advanced unresectable disease as well as an incidence of unrecognized metastases. The majority of patients have a median survival with treatment of less than 6 months. Even for those seemingly fortunate enough to have early-stage local and resectable disease, the 5-year survival is only 20% after resection (1). Therefore, pancreatic cancer is a refractory cancer having poor prognosis.

MUC5AC is a member of the secreted mucin family and is expressed as secretory mucin from goblet cells of the stomach, airways and cervical secretion. These cover the epithelium and provide a lubricating barrier that protects the mucosal surface. On the other hand, it is overexpressed as a membrane-bound type in the ductal region of human pancreatic cancer, while remaining undetectable in the normal pancreas. However, there have been few reports on the function of MUC5AC in pancreatic cancer (2-4).

The dominant view of polymorphonuclear neutrophils (PMNs) is that they are of the most abundant and short-lived in total circulating blood leukocytes and their cytoplasm has highly developed cytomatrices and granules containing microbicidal proteins and digestive enzymes. They provide the first-line of defense against various infections, are potent effectors of inflammation, and release chemotactic factors that lead to the recruitment of non-specific and specific immune effectors (5). Studies on the immunological mechanisms have focused mainly on the function of lymphocytes and monocytes/macrophages as important mediators of the host response. However, PMNs are increasingly recognized as an important effector cell population for the rejection of malignant tumors *in vivo*, including Fas ligand-mediated apoptosis, antibody-dependent cellular cytotoxicity (ADCC), direct cell killing by H_2O_2 and superoxide and calprotectin (6,7).

The antitumor molecule TNF-related apoptosis-inducing ligand (TRAIL) has been reported previously (8,9) and is part of the TNF superfamily member, is expressed in a broad range of cells including activated T cells, B cells, natural killer cells, dendritic cells, monocytes and activated neutrophils, and exerts great antitumor activity. It is known that TRAIL is highly expressed on neutrophils selectively inducing apoptosis. TRAIL exerts its activity by interacting with a complex system of 2 death receptors (DRs) (DR4/TRAIL-R1 and DR5/TRAIL-R2) and 3 decoy receptors (DcRs) [DcR1/TRAIL-R3, DcR2/TRAIL-R4

Correspondence to: Dr Tetsuji Sawada, Department of Surgical Oncology, Osaka City University Graduate School of Medicine, 1-4-3 Asahi-machi, Abeno-ku, Osaka 545-8585, Japan
E-mail: t_sawada@osaka-ekisaikai.jp

Key words: MUC5AC, mucin, pancreatic cancer, short interfering RNA, TNF-related apoptosis-inducing ligand, apoptosis

and osteoprotegerin (OPG)]. Although these receptors are characterized by high sequence homology in their extracellular domains, only DR4/TRAIL-R1 and DR5/TRAIL-R2 contain a functionally active death domain that allows an apoptotic response by TRAIL stimulation (10,11). Some correlations between TRAIL sensitivity and receptor expression have been reported in various tumor cells. TRAIL only acts on cancer cells, it does not act on normal cells. Although there is a theory that this reason is due to a difference in expression levels of death receptors and decoy receptors on these cells, the detailed mechanisms are not known. In our previous study, when MUC5AC-expressing pancreatic cancer cells were knocked down for MUC5AC by specific siRNA, cell survival, proliferation, and morphology *in vitro* were the same as control cells. However, their tumor growth in *in vivo* xenograft studies was significantly lower than that of control cells and most infiltrated leukocytes, particularly neutrophils and B cells, were observed to be accumulated into its tumor challenged site. Moreover, a greater number of antibodies against cancer cells were found in the blood of SW1990/si-MUC5AC cell-challenged mice than that of SW1990/si-mock cell-challenged mice. As a result, it appeared that the tumorigenicity and growth of MUC5AC knockdown cells were significantly lower than that of control cells (12).

In the present study, we assessed the mechanisms of MUC5AC on these immune cells using the neutrophil depletion model by anti-Gr-1 mAb and SCID mice in which B and T cells were depleted. Furthermore, we focused on the anti-tumor effects of neutrophils and hypothesized that MUC5AC was able to inhibit apoptosis via TRAIL signaling pathways. To investigate the function of MUC5AC in pancreatic cancer, we evaluated whether or not MUC5AC knockdown would increase TRAIL responsiveness such as the expression of TRAIL receptor and the effects on apoptosis signaling pathways in pancreatic cancer cells.

Materials and methods

Reagents. Recombinant human TRAIL was purchased from PeproTech GmbH (Paris, France). The tetrapeptide caspase inhibitor z-VAD-fmk was obtained from R&D Systems (Minneapolis, MN). The rat anti-mouse Gr-1 monoclonal antibody used for deplete murine neutrophils was from BD Pharmingen Inc. (San Diego, CA). GeneJuice used for siRNA transfection was purchased from Merck (Darmstadt, Germany).

Animals. Specific-pathogen-free female BALB/c-nu/nu mice (nude mice) and C.B17-scid/scid mice (SCID mice) purchased from Charles River Japan Inc. (Kanagawa, Japan) were acclimatized and then used in experiments at the age of six weeks. The experimental design was approved by the Ethics Committee on Animal Experiments of the Biomedical Research Laboratories of Kureha Corp., and mice were treated in accordance with the guidelines of the committee. All animals were allowed free access to sterilized CE-2 food (Oriental Yeast, Tokyo, Japan) and sterilized tap water. Mice were bred at 25±2°C, a humidity of 55±7%, laminar flow, and under a 12 h light/12 h dark cycle at 150-300 lux. To maintain a uniform environment, noise was carefully avoided and only experimental staff and keepers were allowed into the animal room.

Cell culture conditions. SW1990 was cultured in Dulbecco's modified Eagle's medium (DMEM; Invitrogen Corporation, San Diego, CA) supplemented with 10% fetal bovine serum (FBS; Biowest, Nuaill, France), 50 IU/ml penicillin and 50 μg/ml streptomycin. Cells were grown at 37°C with 5% CO_2 in a humidified atmosphere and passaged before they reached confluency using 0.25% (w/v) trypsin solution containing 0.04% (w/v) EDTA.

Construction of siRNA-MUC5AC and establishing the stable expression cell line. The MUC5AC siRNA target sequence 5'-TTTGAGAGACGAAGGATAC-3' was cloned to generate a stable siRNA expressing construct into the p*Silencer* 3.1-H1 neo vector (Ambion Inc., Austin, TX) as described previously (12). SW1990 cells were transfected with p*Silencer*/si-MUC5AC as a target or p*Silencer*/si-mock as a control using GeneJuice according to the manufacturer's instructions. SW1990 cells were selected by culturing in the presence of geneticin at 600 μg/ml. The efficiency of MUC5AC-knockdown was tested through RT-PCR and FACS analysis (data not shown).

Preparation of neutrophil-depleted mice. Neutrophils were depleted from nude mice using anti-Gr-1 mAb. Anti-Gr-1 mAb was treated at single doses of 100 μg/mice via i.p. injection on days -1, 4, 9, 14, 19, 24, 29, 34 and 39. The depletion of neutrophils was determined before tumor cell implantation by a flow cytometer (13).

Tumorigenicity assay in xenograft models. Cells were implanted subcutaneously (s.c.) at $1x10^7$/mice on the flank of nude mice or SCID mice. Tumor volumes were measured at least once a week. For the determination of tumor volume, two bisecting diameters of each tumor were measured by slide calipers and tumor volumes were calculated using the following formula: tumor volume = length x $(\text{width})^2$ x 0.5236. Eight mice were used for each cell line. Tumor growth curves were plotted as the mean volume ± standard error (SE).

Apoptosis assays. SW1990/si-MUC5AC cells and SW1990/si-mock cells ($2x10^3$ cells/100 μl) were cultured in 96-well plates in medium containing recombinant human TRAIL at fixed concentrations. Cell proliferation was evaluated by the MTT assay as previously described (12). The pan-caspase inhibitor z-VAD-fmk was dosed at 10 μM before 1 h of TRAIL treatment.

Human apoptosis array. The expression profile of apoptosis-related proteins was detected and analyzed using a Proteome Profiler™ (R&D Systems Inc.) according to the manufacturer's instructions. Briefly, protein lysates (500 μg) from SW1990/si-MUC5AC cells and SW1990/si-mock cells were loaded onto an array membrane blocked with blocking reagent. The membrane was incubated overnight at 4°C, washed thrice with TBST, and then incubated with a detection antibody cocktail for 1 h. After three TBST washes,

spots were visualized by a chemiluminescence assay and the average density of duplicate spots was recorded.

Production of IL-8. SW1990/si-MUC5AC cells and SW1990/si-mock cells (10^4 cells/100 μl) were cultured in 96-well plates for 2 or 4 days. Culture supernatants were collected and measured using a human IL-8 ELISA kit (RayBiotech Inc., Norcross, GA), as directed by the manufacturer.

Statistical analysis. All data are expressed as the means ± SE. Statistical significance was determined by the Student's t-test. P-values <0.05 were considered significant.

Results

Effects of MUC5AC on immunocytes. Previous studies have demonstrated that the tumor growth of MUC5AC-knockdown cells is markedly suppressed when they are subcutaneously implanted into a nude mouse. Furthermore, neutrophils and B cells accumulated in the tumor (12). Thus, in the present study, we investigated the effects of neutrophils and B cells on the tumor growth of MUC5AC-expressing cells and the immune evasion mechanism through MUC5AC.

First, to examine the involvement of B cells on the tumor growth of MUC5AC-expressing cells, we investigated the tumor growth of MUC5AC-expressing and MUC5AC-knockdown cells in SCID mice. SW1990/si-MUC5AC or SW1990/si-mock cells were implanted subcutaneously into SCID mice at $1x10^7$ cells/mice and then tumor volume was assessed. If B cells act directly on the antitumor effects of MUC5AC-knockdown-challenged mice, MUC5AC-knockdown cells should grow comparably to MUC5AC-expressing cells. However, the tumor volume of SW1990/si-mock cells increased over time, while that of SW1990/si-MUC5AC cells barely increased and little tumor growth was observed (Fig. 1A).

Subsequently, to examine the involvement of MUC5AC on the antitumor effects of neutrophils, 100 μg of anti-Gr-1 antibody was administered once every five days to a nude mouse to deplete neutrophils. Neutrophil depletion was confirmed by FACS before tumor implantation (data not shown). SW1990/si-MUC5AC or SW1990/si-mock cells were implanted subcutaneously at $1x10^7$ cells/nude mouse, and then tumor volume was assessed. The tumor growth of SW1990/si-MUC5AC cells was barely observed in the presence of neutrophils (Fig. 1B). However, tumor growth recovered to the same level as SW1990/si-mock cells when neutrophils were depleted with an anti-Gr-1 antibody (Fig. 1C).

MUC5AC suppresses IL-8 production of tumor cells. IL-8 produced by peripheral tissue cells and activated neutrophils is involved in the migration of neutrophils into the tissue (8). Hence, the amounts of *in vitro* IL-8 production were determined in SW1990/si-MUC5AC and SW1990/si-mock cells. IL-8 concentrations in the supernatants of SW1990/si-MUC5AC and SW1990/si-mock cells were 1,529 and 179 ng/ml on day 2 and 4,100 and 1,094 ng/ml on day 4, respectively. Suppressed MUC5AC expression significantly increased IL-8 production (Fig. 2).

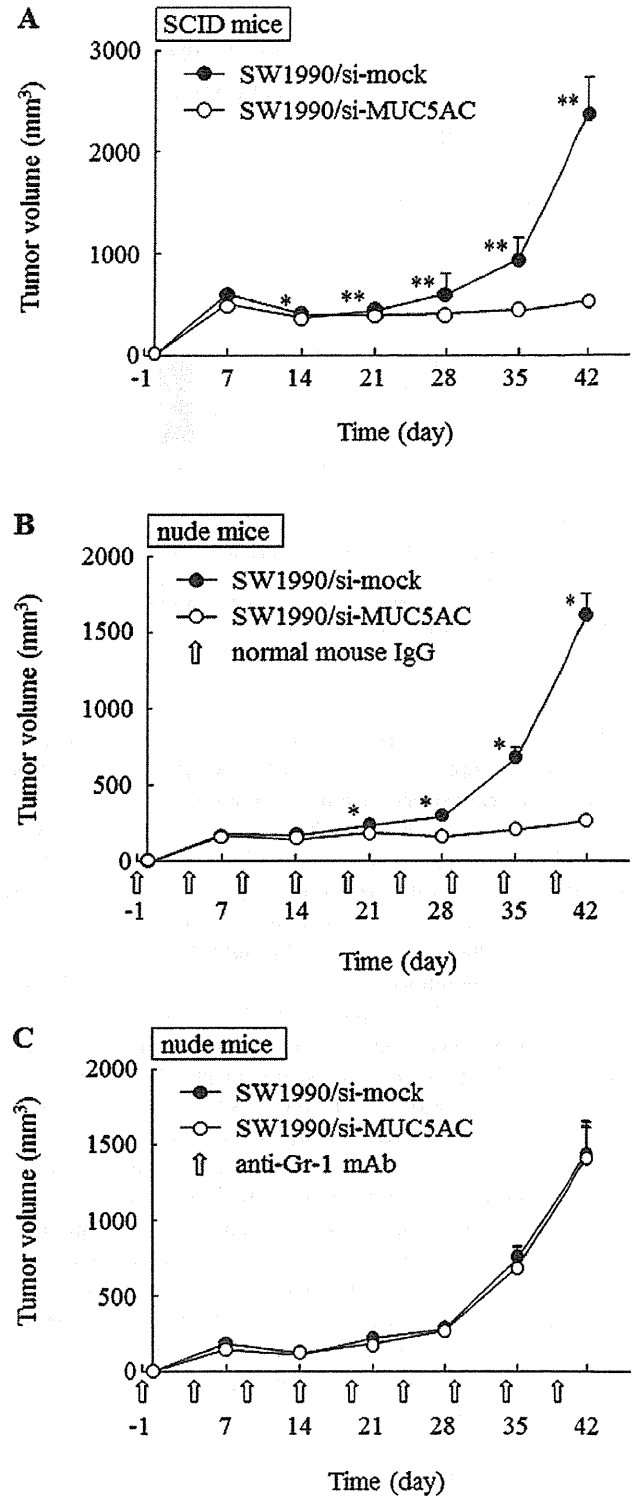

Figure 1. MUC5AC suppresses the antitumor processes of neutrophils. (A) Tumor growth curves of SW1990/si-mock cells (filled circles) and SW1990/si-MUC5AC cells (open circle). Cells were s.c. implanted with $1x10^7$ cells into SCID mice on day 0. (B) Tumor growth curves of SW1990/si-mock cells (filled circles) and SW1990/si-MUC5AC cells (open circle) in normal mouse IgG-treated nude mice. (C) Tumor growth curves of SW1990/si-mock cells (filled circles) and SW1990/si-MUC5AC cells (open circle) in anti-Gr-1 mAb-treated mice. Cells were s.c. implanted with $1x10^7$ cells into nude mice on day 0. Mice were monitored for tumor formation until 42 days and tumor sizes were measured on indicated days. These experiments were performed at least twice and representative data are shown. Points, tumor volume of 8 mice for each group; bars, SE. $^*P<0.05$ and $^{**}P<0.001$.

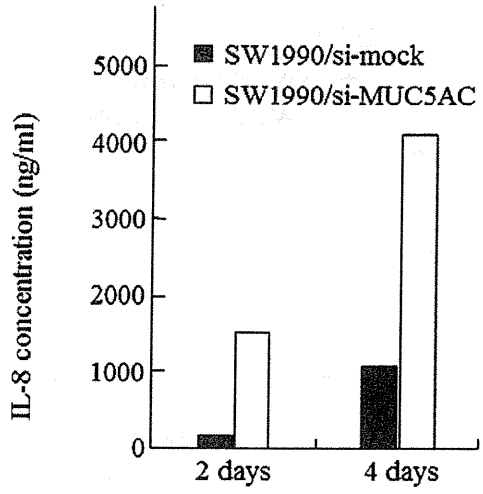

Figure 2. Knockdown of MUC5AC stimulates IL-8 production in pancreatic cancer cells. Cells (10^4 cells/100 μl) were cultured in 96-well plates for 2 or 4 days. Culture supernatants were collected and measured using a human IL-8 ELISA kit. Results were averaged from 3 separate experiments. One representative of at least three similar experiments is shown.

MUC5AC inhibits TRAIL-induced apoptosis. It is known that activated neutrophils produced TRAIL, which in turn, induced apoptosis of cancer cells via its death receptors. Therefore, we evaluated cell viability after TRAIL treatment by the MTT assay. The correlation between the dose of TRAIL and cell growth inhibition is illustrated in Fig. 3A. Our previous reports show that no difference in cell proliferation was observed between SW1990/si-MUC5AC cells and SW1990/si-mock cells under normal conditions *in vitro* (12). After 12 h of TRAIL treatment, cell death was induced in SW1990/si-MUC5AC cells in a dose-dependent manner. In this condition, the IC_{50} value of TRAIL was 5.8 ng/ml. In contrast, treatment of SW1990/si-mock cells at a concentration of TRAIL up to 100 ng/ml resulted in <10% cell death. Concerning cell morphologic changes, SW1990/si-MUC5AC cells were rounded and floating in the medium, while SW1990/si-mock cells still formed a typical epithelioid monolayer at a TRAIL concentration of 100 ng/ml for 4 h (Fig. 3B). Consequently, to examine whether caspases were involved in TRAIL-induced apoptosis in SW1990/si-MUC5AC cells, either the pan-caspase inhibitor z-VAD-fmk (10 μM) or a vehicle control was added to the culture 1 h before TRAIL treatment (10 ng/ml, 4 h). The results indicated that z-VAD-fmk completely blocked TRAIL-induced apoptosis and caspase activation is a required signal event for TRAIL-induced apoptosis. As shown in Fig. 3C, the percentage of cell viability in SW1990/si-MUC5AC cells by the DMSO vehicle control was 92 and TRAIL treatment was 47% in SW1990/si-MUC5AC cells. In contrast, pretreatment of SW1990/si-MUC5AC cells with z-VAD-fmk followed by TRAIL treatment significantly increased cell viability to 93%.

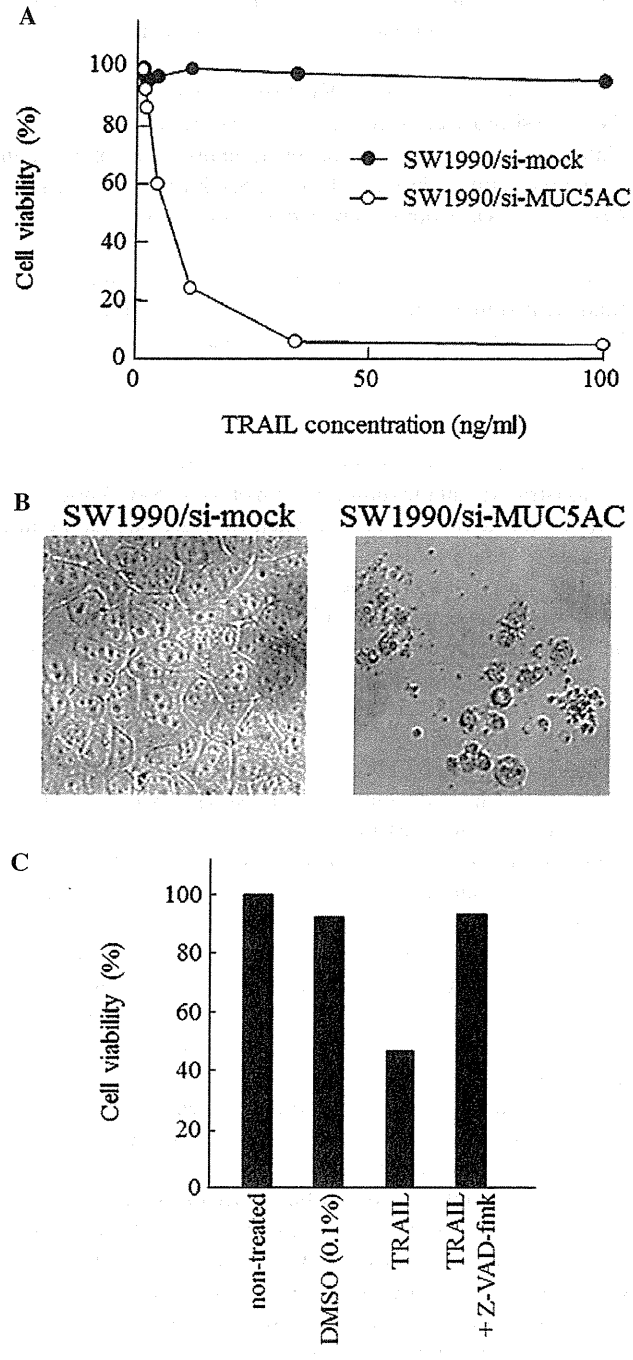

Figure 3. TRAIL induced-apoptosis is stimulated by knockdown of MUC5AC. (A) Cells ($2x10^3$ cells/100 μl) were cultured in 96-well plates in medium containing recombinant human TRAIL at 0-100 μg/ml. After 12 h, cell proliferation was evaluated by the MTT assay. (B) Cells were treated with 100 ng/ml of TRAIL for 4 h. Cells were photographed under a phase-contrast microscope. The representative of three independent experiments is shown. (C) Cells ($2x10^3$ cells/100 μl) were cultured in 96-well plates in medium containing the pan-caspase inhibitor z-VAD-fmk at a dose of 10 μM for 1 h. Twenty ng/ml of TRAIL was treated for 4 h. Cell numbers were determined by the MTT assay.

Analysis of the apoptosis suppression mechanism of MUC5AC using an apoptosis array. As described above, MUC5AC knockdown with siRNA induced apoptosis mediated by TRAIL. Then, to examine differences in the apoptotic signal between SW1990/si-MUC5AC and SW1990/si-mock cells, protein levels relating to apoptosis after the addition of TRAIL to the cells were analyzed using an apoptosis array. Cells were treated with 10 ng/ml of TRAIL for 4 h. The signal intensities in the apoptosis array (Fig. 4A) were digitized and normalized for the positive control value (Fig. 4B). The vehicle control

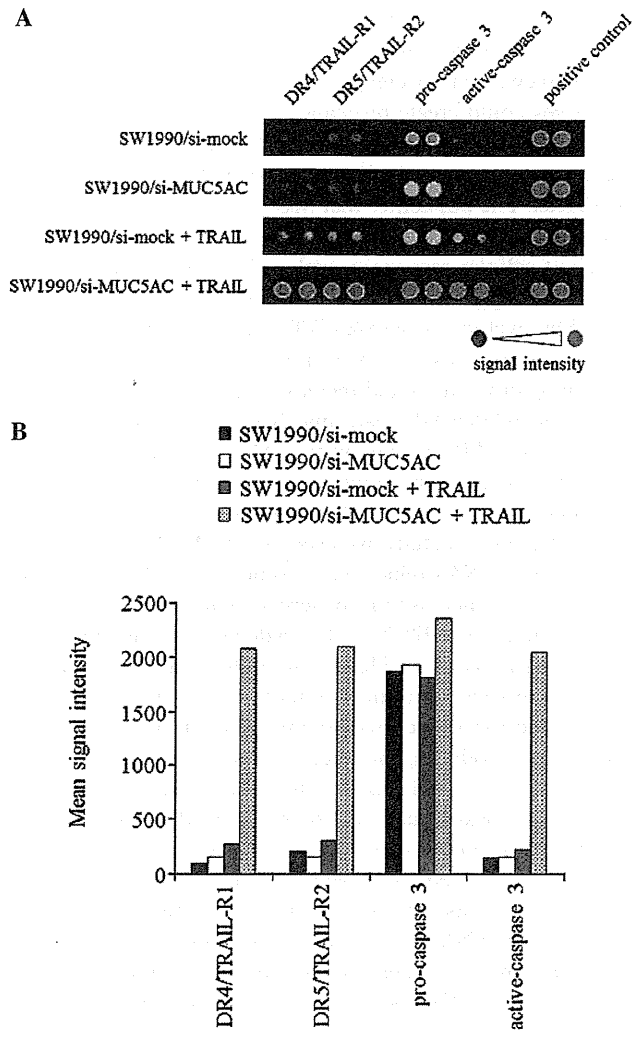

Figure 4. Apoptosis array analysis of pancreatic cancer cells upon knockdown of MUC5AC. (A) Total protein lysates (500 μg) from SW1990/si-mock cells and SW1990/si-MUC5AC cells were analyzed using Proteome Profiler™. Depicted are representative images of chemiluminescence signals with differences in signal intensities between si-MUC5AC and si-mock cells. One representative of duplicate experiments is shown. (B) Densitometric analysis of apoptosis array blots. Values relative to DR4/TRAIL-R1 expression levels of SW1990/si-mock values set to 100. Means are averaged from 2 spots.

for SW1990/si-MUC5AC cells showed weak expression of TRAIL receptors (DR4/TRAIL-R1 and DR5/TRAIL-R2) and active-caspase 3 and strong expression of pro-caspase 3 (active-caspase 3 precursor). The same expression patterns were observed for SW1990/si-mock cells. However, the addition of TRAIL induced an enhancement in the expression of DR4/TRAIL-R1 and DR5/TRAIL-R2 in SW1990/si-MUC5AC cells. Additionally, a significant increase in active-caspase 3 expression was observed. On the other hand, TRAIL had no effect on DR4/TRAIL-R1 and DR5/TRAIL-R2 expressions in SW1990/si-mock cells.

Discussion

Mucins are classified generally into two groups: a secretory type and membrane-bound type. Secretory mucins include MUC2, MUC5AC, MUC5B and MUC6. These mucins are called 11p15.5 mucin because they are located on human chromosome 11p15.5 and are structurally similar. On the other hand, membrane-bound mucins include MUC1, MUC3A, MUC3B, MUC4, MUC11, MUC12 and MUC13. All these mucins have transmembrane domains. MUC3A, MUC3B, MUC11 and MUC12 are located on chromosome 7q22, while MUC4 and MUC13 are located on chromosome 3q29. MUC7 and MUC8 belong to neither of the above groups and have no mutual similarity (3,14). The core protein of a mucin molecule has a characteristic repetitive sequence. The repetitive sequence, rich in Thr and Ser, is frequently bound to a mucin-type sugar chain. Mucin-type sugar chains generally consist of N-acetylgalactosamine, N-acetylglucosamine, galactose, fucose and sialic acid. Sugar chains account for 50-80% or above of the molecular weight of mucin, giving it various properties including viscosity, a water-holding capacity and proteinase resistance. Thus, the sugar chain structure of mucin, which is varied quantitatively and qualitatively with malignant transformations, is likely to be involved in altered adhesion during metastasis and evasion from immune cells. However, the detailed mechanisms remain unclear.

We established MUC5AC-knockdown cells using siRNA and have previously reported analysis of the functions of MUC5AC in cancer cells (12). A stable human pancreatic cancer cell line, SW1990/si-MUC5AC, obtained by introducing si-MUC5AC into a parent SW1990, was almost equal to the control cells, SW1990/si-mock, regarding *in vitro* morphology, proliferation and infiltration capacity. However, an *in vivo* subcutaneously implanted model yielded results completely different between SW1990/si-MUC5AC and SW1990/si-mock cells. SW1990/si-mock cells caused continuous rapid tumor growth, whereas SW1990/si-MUC5AC cells caused only slight tumor growth when they were subcutaneously implanted into nude mice. Furthermore, the amounts of immune cells, including neutrophils and B cells, existed in the tumor derived from SW1990/si-MUC5AC cells. Tumor-specific antibodies also existed in the serum. This suggests that MUC5AC-expressing cells may suppress immune cells to evade the immune system, thereby playing an important role in creating an environment to facilitate cancer cell survival.

Neutrophils are characterized by immunity against bacteria, such as direct phagocytosis of bacteria and opsonophagocytosis of encapsulated bacteria. According to previous reports, neutrophils also have antitumor effects. The antitumor effects of neutrophils are reportedly caused by a number of mechanisms including ADCC activity through a tumor-specific antibody, apoptosis induction mediated by TRAIL (15-19). Furthermore, inhibition of tumor growth by IL-12 was reduced when neutrophils were depleted in a mouse model of prostate cancer (20). PMNs are the predominant effector cell population for the killing of breast cancer cells in the presence of HER-2/neu monoclonal antibody (6). In addition, PMN-mediated ADCC has been reported to contribute to the efficacy of the antitumoral antibody rituximab and trastuzumab (13,21,22).

Additionally, TRAIL is expressed at significantly higher levels in neutrophils than in other immune cells. TRAIL was isolated in 1995 as a cytokine that induces apoptosis and has a TNF-family analogous sequence (23). TRAIL is ~30 kDa type II cell surface protein consisting of 281 amino acids and is